Plasma mass separation

S. J. Zweben,[1] R. Gueroult,[2] and N. J. Fisch[1]
[1]*Princeton Plasma Physics Laboratory, Princeton, New Jersey 08540, USA*
[2]*Laplace, Universite de Toulouse, CNRS, 31062 Toulouse, France*

(Received 5 June 2018; accepted 15 August 2018; published online 12 September 2018)

This tutorial describes mechanisms for separating ions in a plasma device with respect to their atomic or molecular mass for practical applications. The focus here is not on separating isotopes of a single atomic species but rather on systems with a much lower mass resolution and a higher throughput. These separation mechanisms include ion gyro-orbit separation, drift-orbit separation, vacuum arc centrifugation, steady-state rotating plasmas, and several other geometries. Generic physics issues are discussed such as the ion charge state, neutrals and molecules, collisions, radiation loss, and electric fields and fluctuations. Generic technology issues are also discussed such as plasma sources and ion heating, and suggestions are made for future research. *Published by AIP Publishing.*
https://doi.org/10.1063/1.5042845

I. INTRODUCTION

This tutorial describes mechanisms for separating ions in a plasma device with respect to their atomic or molecular mass for practical applications. As a tutorial, this paper aims to explain (with an educational perspective) the principles and techniques in this field and to communicate a broad overview of the objectives, results, and open questions.

Sec. I A describes the motivations and goals in this field, Sec. I B reviews the history of previous experiments, and Sec. I C describes a generic device and its approximate parameters. Mechanisms for ion mass separation are discussed in Sec. II, physics and technology issues are described in Secs. III and IV, respectively, and future research directions are discussed in Sec. V.

A. Motivations and goals

The focus of this tutorial will *not* be on separating isotopes of a single atomic species, as done originally using calutrons in WWII[1] but rather on low mass resolution ion separation at a higher throughput than the existing isotope separation methods. If the physics and technology of an efficient high throughput plasma mass separation device can be demonstrated, this technique could provide a new and valuable tool to supplement conventional chemical and physical separation methods, which have widespread application in science and industry.[2]

Three possible applications of low-resolution plasma mass separation are shown in Table I, based on the discussion in Ref. 3. Each of these is driven by difficulties or high costs associated with more conventional methods of chemical or physical separation. Also shown for reference in Table I is a typical isotope mass separation device, based on the review in Ref. 4.

The first and most ambitious of these applications is nuclear waste remediation for sites like Hanford (USA), at which there is presently $\sim 10^8$ kg of mixed nuclear and chemical waste stored in 177 underground tanks left over from the plutonium production processes. The goal of plasma mass separation would be to pretreat the waste to coarsely separate the high-mass radioactive components with atomic masses of roughly $M > 80$ from the low-mass non-radioactive components with $M < 80$. This would reduce the volume of high-level radioactive waste which needs to be buried deep underground, which should reduce the cost of remediation. Given a 30 year timetable, this implies a throughput of $\sim$10–100 g/s, which is an ambitious goal which would probably require multiple plasma separation devices running in parallel. The mass separation factor needed for nuclear waste is modest, with a separation factor of $S = (f_A/(1-f_A))/(f_B/(1-f_B)) \sim 2$–4, where f_A and f_B are the fractional abundances of the high mass components after and before separation. This is in part because of the fact that the mass fraction of radioactive elements is already small in the feed. Given the large projected cost of the Hanford project (or perhaps a similar application to the Fukushima cleanup in Japan), a cost goal for this plasma pretreatment could be up to $\sim$\$100/kg. More details on this application are given in Ref. 5.

The second application in Table II involves the separation of minor actinides ($M = 227$–259) from lanthanides ($M = 139$–173), after the chemical extraction of 99.9% of uranium and plutonium from the spent nuclear fuel.[4,6–8] The transmutation of the long-lived minor actinides into shorter lived or stable elements is considered as a way to decrease the mandatory storage time of remaining nuclear waste to a few hundred years, in place of several thousand years. A prerequisite to this step consists in the separation of lanthanides because of their large neutron capture cross-section. From a chemical standpoint, this separation is made particularly difficult by the chemical similarities existing between the two groups of elements.

The third application involves the plasma separation of rare earth elements (REEs), with the atomic mass over 140, from lighter elements in the recycling of NdFeB magnets.[9] This application is driven by the interest for REE production pathways which could alleviate supply risks while limiting the environmental impact associated with mining. Since NdFeB magnets contain over 25% in mass of REEs, separating out

TABLE I. Goals for plasma mass separation.

Application	Mass cutoff (amu)	Separation factor (see the text)	Throughput (g/s)
Nuclear waste	∼80	∼2–4	∼10–100
Spent nuclear fuel	∼200	∼1000	∼0.01–1
Rare earth recycling	∼100	∼100	∼1–100
Isotope separation	ΔM=1	variable	10^{-4}–10^{-3}

rare-earth elements in end-of-life magnets holds promise for REE urban mining. However, chemical recycling techniques are similar to ore processing techniques and hence often have a significant environmental footprint.

An important issue for this technology is the incompleteness of any plasma mass separation process, particularly for nuclear waste applications where the separation factor may be relatively low. In practice, the requirements for separation will be set by the regulations or economics of the specific application; for example, shallow burial of low-level nuclear waste can tolerate some small level of radioactive materials in the low-mass output stream. This points to the need for careful chemical/radiological analysis of the device output to determine its actual composition, which can of course vary with the input composition and device performance. If the output is insufficiently separated, it can in principle be recycled back through the device for improved separation.

Another significant goal for research on plasma mass separation is to explore the basic physics of what might be called *differential ion confinement* in magnetized plasma devices. For example, extraction of high mass impurities from magnetic fusion devices would be helpful, and there may be analogies to species segregation in industrial processing or space plasmas. There are of course many aspects of the plasma stability and atomic physics in these devices that are still not well understood, as discussed in Sec. III.

A successful demonstration of a universal plasma mass separator would probably generate further applications, perhaps analogous to the widespread use of atmospheric pressure plasma torches for waste treatment.[10] However, the plasma mass separators discussed here will have some practical constraints: they operate under high vacuum, they require a minimum energy investment to ionize and heat the atoms, and their throughput is limited by their low density with respect to atmospheric pressure. Some of these physics and technology issues are discussed further in Secs. III and IV, respectively.

TABLE II. Previous experiments on plasma mass separation.

Device (location)	Working species	Year(s)
Calutron (Berkley, ORNL)	U isotopes	1941–1998
FI torus (Sweden)	H/Ar	1966–1971
ICRH (US, Russia, France)	Many isotopes/elements	1976–present
Plasma centrifuge (Yale)	Metal isotopes and elements	1980–1987
Vacuum arc centrifuge (Australia)	Cu/Zn and their isotopes	1989–1999
PCEN vacuum arc centrifuge (Brazil)	C, Al, Mg, Zn, Cd, Pb, etc.	1987–1998
Archimedes filter (San Diego)	Xe/Ar and Cu/Ag/Au?	1998–2005
Linear device with electrodes (Kyushu)	Ar and Xe	2007
POMS-E-3 (Irkutsk)	N, Ar, and Kr	2010–present
Vacuum arc separator (Irkutsk)	Ni, Cr, Fe, and W	2011–2015
PMFX (PPPL)	Ar/Kr	2013–2014
SNF separator (JIHT Moscow)	U, Gd, and He	2013–present

B. Experimental history

The mass distribution of atoms and molecules can be precisely analyzed for small samples using various types of mass spectrometers.[11,12] These devices can ionize and analyze a wide range of masses with an accuracy of ∼1 amu, even including large biological molecules, using sophisticated techniques such as quadrupole mass analysis, plasma or laser desorption mass spectroscopy, inductively coupled plasma mass spectroscopy, glow discharge mass spectroscopy, or Fourier transform ion cyclotron resonance mass spectroscopy. Conventional mass spectrometers often use a plasma to generate the ions but measure the charge/mass ratio of the ions *without* a neutralizing electron background. Thus, space-charge effects constrain their throughput to be microscopic ($\lesssim 1\ \mu$g/s), and so, they have limited relevance for the medium-to-high throughput plasma-based mechanisms discussed in this paper.

A partial list of devices which have been used for plasma-based ion mass separation is shown in Table II. Note that the information about some of these experiments is limited due to classification or proprietary interest, and not all plasma separation devices are covered.

The first medium-throughput mass separation of ions was done using calutrons in the Manhattan project.[1,13–15] Natural uranium was turned into gas molecules, which were then singly ionized by an electron beam and electrostatically accelerated to form multiple ∼35 keV ion beams within a magnetic field of B ∼ 5 kG. The U^{235} and U^{238} isotopes were then separated using their 0.6% different ion gyroradii (typically ∼100 cm), and ∼10% of the ionized atoms were recovered using mechanical slits and deposition on graphite receivers. The total uranium throughput was apparently $\sim 10^{-3}$ g/s per calutron, with ∼1000 calutrons at ORNL by 1945. Since then some remaining calutrons have been used for producing ∼10–100 of grams/year of stable isotopes of many different elements for medical and industrial purposes.[16] An alternative optically pumped magnetic separation device was also recently developed for isotope separation.[17]

The first experiments on ion mass separation in a thermal plasma were done in Sweden in 1966–71 using a rotating plasma in a toroidal magnetic chamber with B ∼ 6000 G,[18] as shown in the second entry in Table II. This was motivated in part by the theory of gas centrifuges, in which radial mass separation was expected at high rotation speeds. The gases used were H, D, Ne, and Ar, and gaseous samples were extracted from inside the plasma with a collector probe at various locations and analyzed using a mass spectrometer well after the ∼10 ms plasma discharges. The relative concentration ratio of Ar/H_2 was observed to increase with the radius of the sampling probe, at least qualitatively in agreement with the expected centrifugal separation process.

The third entry in Table II is ion cyclotron resonance (ICR) experiments for isotope separation, such as implemented in a private company TRW starting around 1976.[19] The first results showed selective ICR acceleration of ions in a linear Q-machine at a magnetic field of $B \sim 2.5$ kG, densities of $\leq 10^{11}$ cm^{-3}, and a temperature of $T_e \sim 0.2$ eV, along with a significant variation in the measured ≤ 50 eV ion populations of K^{39} vs. K^{41} as the magnetic field was varied slightly. Many other ICR separation experiments have been done in the US, France, and Russia to resonantly increase the gyroradius of various elements and isotopes in a linear magnetic field configuration and to collect the separated ions using carefully designed baffles and biased electrodes at the far end. Extensive reviews of such experiments are given in Refs. 4, 7, and 20, including large devices intended for the separation of spent nuclear fuel. These experiments have successfully separated many ion species and isotopes and seem to be considerably more efficient than calutrons in terms of cost per gram. The measured isotope production rates have been $\leq 10^{-3}$ g/s of the Ni^{62} isotope at TRW and $\leq 10^{-5}$ g/s of Li^6 at Kurchatov, and the estimated (potential) production rate for Ca^{48} is 5 kg/year.[4]

The next entry in Table II is the plasma centrifuge developed by Krishnan *et al*. during 1980–87[21–23] and later refined by Australian[24–26] and Brazilian[27–30] groups. The original device has a metal cathode electrode as the source of the material to be separated, located at one end of a ~1–2 m long chamber with a magnetic field of $B \sim 7$ kG.[21] A metal vapor plasma is created by applying a ~4 kV voltage to the cathode with respect to the chamber wall, which formed a ~5 kA arc for ~1 ms. An azimuthal plasma rotation was created by the self-consistent electric fields with speeds of up to $V_\theta \sim 5 \times 10^6$ cm/s. The metallic cathode elements were deposited at the far end of the device, and their mass spectrum was measured using SIMS and x-ray photoelectron spectroscopy. The radial separation of Al/Ti and Cu/Ni mixtures with a separation factor of ~2 and the enrichment of heavy isotopes of Mg, Ca, and Tl by a factor of ~2 were observed, roughly consistent with a fluid model for the vacuum-arc centrifuge. The energy cost for separation in this device was estimated to be 7×10^4 eV/atom[21] or 100 MJ/g at $A = 70$, which translates into ~$5000/kg, which is too high for the applications of Table I. The experimental results in Australia and Brazil were at least qualitatively similar to the Yale results. Large coherent fluctuations were apparently observed in all vacuum arc centrifuges, and a theoretical analysis of plasma instability in a vacuum arc centrifuge was done jointly by the Australian and Brazilian groups.[30] A critical review of vacuum arc centrifuges was recently given in Ref. 31.

One of the largest experimental efforts on plasma mass separation since WWII was made at the privately funded Archimedes Technology Group in San Diego, circa from 1998–2005, based on a theory of single-particle ion orbit confinement by Ohkawa.[32] Their DEMO device design aimed to process surrogate Hanford nuclear waste with a throughput of $\sim 0.7 \times 10^3$ kg/day with an energy cost per ion of ~0.5 keV/ion,[33–35] which is ~100 times lower than the estimated energy cost for the plasma centrifuge. A linear helicon plasma device was built with a length of 3.9 m, a diameter of 0.4 m, and a magnetic field of $B \leq 1.6$ kG. This plasma was heated with ~3 MW of 6 MHz RF power and driven with end electrodes biased at ≤ 700 V to create a rotating plasma. Data on plasma density profiles with RF but without biasing were published,[36] but no separation measurements were published.

An initial experiment to test the mass separation effect of radial electric fields in a linear magnetized plasma device was done by Shinohara *et al*.[37] A saturation in the azimuthal flow speed was observed in Xe plasmas but not in Ar plasmas, apparently consistent with the mass-dependent orbit loss model of Okhawa. This experiment was done at a very low density of $n \sim 10^{10}$ cm^{-3}, which is appropriate for studying collisionless orbit effects but leads to very low throughput for a given machine size.

A significant experimental effort on plasma mass separation has been ongoing at Irkutsk (Russia) since ~2010. The Paperny group uses a pulsed vacuum arc in a ~200 G curved magnetic field, where the ion gyroradius is comparable to the chamber size. They reported spatial separation of Fe and W ions based on the x-ray fluorescence measurement of metallic films deposited on targets[38] and energy spectra of various ion charge states.[39] The Bardakov group focuses on the POMS concept ("plasma optical mass separation"), involving a region of variable magnetic fields of $B \sim 0.5$ T along with biased electrodes.[40–42] Separation of N, Ar, and Kr in ions was done successfully, although with some overlap of different ion mass flows.[42]

The next entry in Table II is the Plasma Mass Filter Experiment (PMFX), operated at the Princeton Plasma Physics Laboratory from 2013–14.[43] This experiment was based on an existing steady-state linear helicon device with the RF heating of ~1 kW at 13.6 MHz and an axial magnetic field of $B \leq 1$ kG. Three coaxial end electrodes were biased to test the effect of applied electric fields on plasma rotation and noble gas ion separation. Slight differences were measured in the radial profiles of singly ionized Ar vs. Kr lines as a function of biasing, which suggested (but did not prove) differential ion confinement. Subsequent theoretical analysis[44] showed that significant device modifications would be needed to produce ion separation due to the high collisionality in this experiment.

The final entry in Table I represents the work on Spent Nuclear Fuel (SNF) processing at the Joint Institute for High Temperatures in Moscow.[45–50] This comprises theoretical work[45,46] and the design and construction of a separation device with a diameter of 0.9 m, a length of 2.0 m, and a field of $B = 2.1$ kG.[47] Preliminary measurements were made of the electrostatic potential profile in discharges biased with a cathode potential of 1190 V,[48] and a diffuse vacuum arc plasma source was developed which produced ~3 mg/s of metal ions with an average charge of about +1.[49,50] This seems to be the most active plasma separation program at present although no results on separation have been published.

In summary, there have been at least a dozen small-to-medium scale experiments which have explored plasma mass separation in various types of devices around the world for the past 50 years, mainly aimed at isotope separation or

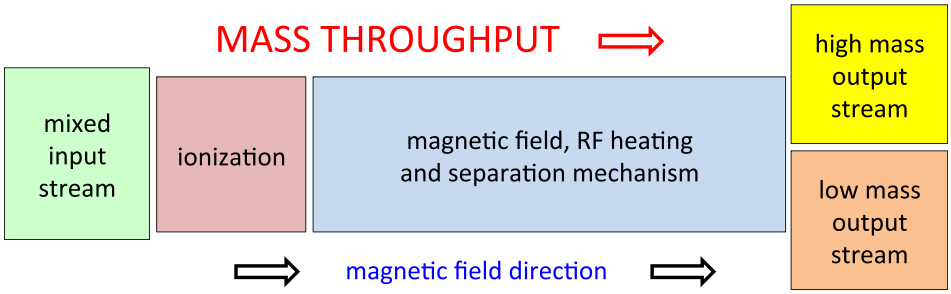

FIG. 1. Generic plasma separation device configuration. The input stream is introduced into the vacuum system and converted into neutral atoms or molecules at the left (green box). Ionization to $Z=1$ is done in the next stage (red box), after which the ions are separated by mass in a magnetic field (blue box). The high and low mass output streams are physically separated and extracted at the right.

spent nuclear fuel reprocessing. Only a few of these are currently active, and although some of them have provided useful quantities of isotopes for defense and medical purposes, none of them appear to be commercially successful. However, there does appear to be considerable scope for new innovations and new applications, as discussed in recent reviews.[3,4,6,7,20,31]

C. Generic plasma separation device

To help introduce the subsequent discussion and orient the reader, we show in Fig. 1 a conceptual design for the type of plasma separation device discussed in this tutorial. The mixed input stream is introduced into the vacuum system in the green section at the left and then singly ionized in the adjacent red section (see Sec. III A). The ionized plasma is directed along a magnetic field of typically $B \sim 10^3$–10^4 G through the central (blue) section, where the plasma is heated and the ions are separated by mass. There will also be some neutral gas in this chamber at a pressure of ~1–10 mTorr (10^{-6} to 10^{-5} bar). At the right side, the ions are physically separated and deposited into either a high-mass stream or a low-mass stream, from which they are extracted. Note that the magnetic field might be curved or variable, and the source and exhaust sections could be in different locations for different types of separation mechanisms. Multiple output streams for various mass ranges are also possible.

Table III shows a set of generic machine and plasma parameters for a device like that in Fig. 1. Approximate values are shown for both an initial small-scale experiment and a practically useful system. For initial experiments, the average ion charge should normally be $\langle Z \rangle = +1$ at an electron temperature of $T_e \sim 1$–2 eV. The electron and ion density would be around $n_e \sim 10^{13}\,\mathrm{cm}^{-3}$, and the neutral (unionized) atom density n_o would be $n_e \sim 10^{14}\,\mathrm{cm}^{-3}$. The maximum possible ion throughput will depend on the ion speed v_i, which depends on the ion temperature T_i. Assuming $T_i = 10$ eV, an average ion mass $A = 40$ (argon), and an ion density of $n_i \sim 10^{13}\,\mathrm{cm}^{-3}$, the *maximum* possible collisionless ion flux (throughput) is roughly $\Gamma \sim {}^1/_2\, n_i v_i \sim 2.5 \times 10^{19}$ ions/(cm^2 s). For an exhaust area of $\sim 10^4$ cm^2, this is equivalent to a mass throughput of ~1–2 g/s, which is not too far from the values shown in Table I. However, the ions are normally collisional at the temperatures and densities shown in Table III, and so, detailed calculations are needed to evaluate the actual throughput.

II. MECHANISMS FOR PLASMA SEPARATION

This section describes several different plasma mechanisms which could be used to separate ions of different masses, some of which have been used in previous plasma separation experiments (Sec. I B). All these mechanisms depend on the ion charge/mass ratio, and so, for effective mass separation, all ions are assumed to have $Z = +1$ (but see Sec. III A). Plasmas are assumed here to be quasi-neutral with $n_e = n_i$, but we do not assume that they are fully ionized, since typically the neutral density is $n_o \geq n_e$. Various generic physics issues (i.e., difficulties) common to most of these separation mechanisms are discussed further in Sec. III.

A. Ion gyro-orbit separation

Perhaps the simplest method for separating ions of different masses in a magnetized plasma is to exploit the geometrical differences in the ion gyroradius with M_i, as used in WWII calutrons. Assuming an ion charge of $Z = +1$, the ion gyroradius is

$$\rho_i = v_i/\omega_{ci} \sim 100\left[M_i(\mathrm{amu})\,T_i(\mathrm{eV})\right]^{1/2}/B\,(\mathrm{Gauss}), \quad (1)$$

where $v_i = (kT_i/M_i)^{1/2}$ is a typical ion velocity at an ion temperature of T_i, B is the magnitude of the magnetic field, and ω_{ci} is the ion cyclotron frequency (radians/s). Note that there will be an order-of-unity variation in the range of gyroradii for each ion species, depending on the angle of the ion with respect to the magnetic field and on the ion velocity within the thermal ion distribution function. Thus, this separation mechanism is not very sharp, at least for thermal ions, and obviously requires ions to complete at least one gyro-orbit without pitch-angle scattering due to collisions (see Sec. III F).

An example of the gyro-orbit separation device is shown in Fig. 2, taken from the excellent review of Dolgolenko and

TABLE III. Generic plasma mass separation device parameters.

Parameter	Initial	Practical
$L_{\|\|}$ (axial length)	1 m	<4 m
a (radial width)	0.2 m	0.2–1 m
$B_{\|\|}$ (magnetic field)	0.2 T	≤1 T
P_{rf} (RF power)	5 kW	100–1000 kW
Z (ion charge)	~1	1–2
M_l (light ion mass)	40 (Ar)	5–70
M_h (heavy ion mass)	84 (Kr)	70–240
n_e (electron density)	$10^{13}\,\mathrm{cm}^{-3}$	10^{12}–$10^{14}\,\mathrm{cm}^{-3}$
n_i (ion density)	$10^{13}\,\mathrm{cm}^{-3}$	10^{12}–$10^{14}\,\mathrm{cm}^{-3}$
n_o (neutral density)	$10^{14}\,\mathrm{cm}^{-3}$	10^{13} –$10^{14}\,\mathrm{cm}^{-3}$
T_e (electron temperature)	1–2 eV	1–5 eV
T_i (ion temperature)	1–10 eV	10–1000 eV

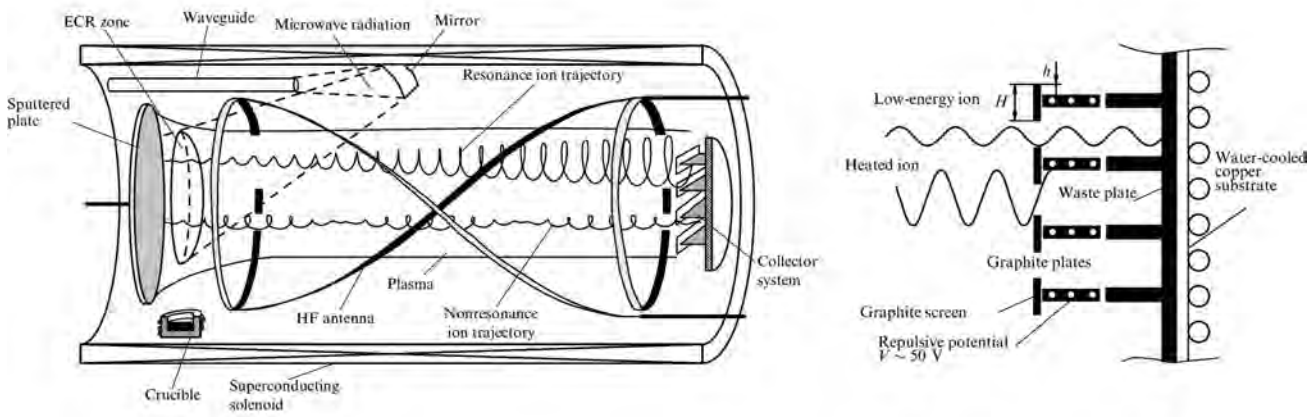

FIG. 2. Example of a gyro-orbit mass separation device. The atoms are created by ion sputtering or a heated crucible (at the left) and singly ionized by ECRH. Selected ions are heated by ICRH antennas in the middle section, and different gyroradii are deposited on the side and end plates at the right. Reprinted with permission from D. A. Dolgolenko and Yu. A. Muromkin, Phys.-Usp. **52**(4), 345–347 (2009). Copyright 2009 Turpion Ltd.

Muromkin of the Kurchatov Institute.[4] This is representative of several ion cyclotron resonance (ICR) isotope separators built in the US, Russia, and France (see Table II). To increase the ion separation in devices of this type, selective ion heating can be done at specific resonant frequencies using ICRH. The resulting spatial separation due to ion gyro-orbit differences can also be supplemented by electrostatic separation due to biasing at the end collectors, as illustrated at the bottom right of Fig. 2.

The source of neutral atoms is either a heated crucible (for volatile materials) or a large sputtering plate biased negatively at 2–4 kV, as shown at the left of Fig. 2. The neutrals are ionized inside an electron cyclotron heating region, aided by electron mirroring between the negative sputtering plate and the main magnetic field. The ions flow into the long solenoid to the right, where ion cyclotron resonant heating is applied using inductive four-phase antennas at 0.1–1 MHz to increase the gyroradius of the selected species. The ions of various gyroradii were collected at the right end by biased plates. The lower gyroradius ions were collected on surfaces directly along B field lines, while the high gyroradius ions were deposited on the sides of these collectors, as shown at the right of Fig. 2. Although this technique was originally designed for isotope separation, it can also be used for the separation of different atomic mass species, e.g., for spent nuclear fuel reprocessing,[7,31] perhaps with multiple RF frequencies and antennae.

The main advantage of this system is its conceptual simplicity, compared for example to the methods below which require large plasma potentials and/or high rotation. The main disadvantage is the difficulty of the ICRH coupling and heating physics, especially at high plasma density and high throughput.[4,7,31] The energy cost of ICRH heating will probably limit the maximum ion energy (and corresponding gyroradius) to $T_i < 1$ keV. A somewhat similar gyroradius separation geometry with radial heavy ion collectors was the basis of the Archimedes proposal[32–36] since their theoretical "band gap" cutoff condition $M_i/Z > eB^2a^2/8V_{dc}$ is equivalent to $\rho_i > a/8$ of Eq. (1), where $E_{rad} = V_{dc}/a$. But for the Archimedes scheme, the ion gyroradius is determined mainly by the azimuthal $E \times B$ rotation speed and not by direct ICRH.

B. Ion drift orbit separation

A second ion mass separation mechanism would exploit the collisionless drift orbit motion of ions in a magnetic field. For example, ions with a gyroradius ρ_i in a magnetic field with the radius of curvature R (with $\rho_i < R$) will drift perpendicular to B and grad-B over many gyro-orbits at an average velocity of $v_\perp = (\rho_i/R)\, v_i$, where v_i is the ion velocity and $\rho_i = v_i/\omega_{ci}$ is the ion gyroradius, which depends on the ion temperature and mass through Eq. (1). Of course, electrons will drift in the opposite direction, thus tending to create an internal electric field which will oppose this drift motion.

An illustration of this scheme is shown in Fig. 3, taken from Ref. 7. The ions created in the source at the left would

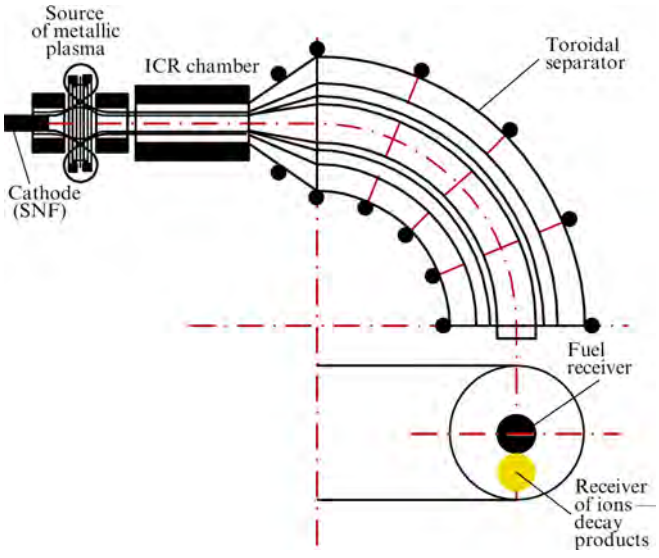

FIG. 3. Example of drift orbit separation. The ions are created and heated at the upper left and transferred to a curved magnetic field section at the upper right. The ion drift orbits are separated according to the mass in the vertical direction (into the page), as shown in the cross-section at the lower right. Reprinted with permission from A. V. Timofeev, Phys.-Usp. **57**(10), 990–1021 (2014). Copyright 2014 Turpion Ltd.

be heated in the linear magnetic field section to increase their temperature and would then drift along the axial magnetic field into the curved magnetic field section, in which they would be separated vertically (as shown at the bottom). The vertical deflection $\delta_\perp$ of an ion with a parallel speed of $\sim v_i$ in a half-torus would be about π times the ion gyroradius and increases with ion mass M_i and ion temperature T_i (assuming an ion charge $Z = +1$) as

$$\delta_\perp \sim (2v_\perp/v_i)\pi R \sim \pi\rho_i \sim 320\left[M_i(\text{amu})\,T_i(\text{eV})\right]^{1/2}/B\,(\text{Gauss}). \quad (2)$$

Note that the ion heating in the proposal of Ref. 7 uses selective ICRH of nuclear ash, in which the orbit drifts are increased for specific ion species to improve the separation efficiency.

Early experiments on plasma transmission through 90° magnetic field bends were done in the US[51] and in Russia[52] using pulsed plasma sources, which showed a reduction in heavy ion impurities as measured using ion energy analyzers after the bend. Further experiments on the ion drift motion were done at Columbia[53] and in Japan[54] using steady-state Q-machines, which showed a short-circuiting of the expected $E \times B$ drift due to nearby conductors and to the electron drift along the magnetic field. The use of a curved magnetic field for separation of ions has been reviewed in the context of plasma processing of spent nuclear fuel,[7] and a related concept of ion separation in a bent magnetic mirror was recently proposed.[55] It might be possible to use permanent magnets to create a curved field, which would reduce the complexity and cost of a plasma mass separation device.

The main advantage of this mechanism is that the ion separation occurs passively without any externally applied electric field. The main difficulty is the tendency for this system to create a self-generated electrical field due to the separation of ions and electrons, which would cause outward $E \times B$ drifts of all species together, thus removing the separation effect. Another difficulty is that the source profile would have to be shaped into horizontal "slits" for the vertical curvature-induced separation to result in spatial separation at the far end. Note that this separation is independent of the radius of field curvature but does require $R > \rho_i$. The separation distance increases with the toroidal angle of the field bend and could potentially be increased using multi-turn orbits inside a vertically elongated torus like a Helimak.[56]

C. Plasma centrifuge (vacuum arc centrifuge)

The separation mechanism of a plasma centrifuge (a.k.a. vacuum arc centrifuge) is similar to that of a liquid or gaseous centrifuge in that more massive particles are forced radially outward by rapid azimuthal rotation. The density profiles of two ion species of different masses were calculated using radial force balance in a two-fluid model for masses M_i with charges Z_i in a plasma rotating with azimuthal $E \times B$ velocity V_θ[21,23,26,57]

$$n_1(r)/n_2(r) = \left[n_1(0)/n_2(0)\right]\exp\left[(Z_1M_2 - Z_2M_1)(V_\theta{}^2/2kT)\right]. \quad (3)$$

The radial separation should be significant if the ions are rotating near $V_\theta \sim V_i \sim c_s$ (i.e., when $T_i \sim T_e$), where heavy $Z = 1$ ions should equilibrate at significantly larger radii. A similar radial mass separation mechanism for high (M,Z) ions has been seen in rapidly rotating tokamak plasmas.[58,59]

An illustration of the original experimental device of this type is shown in Fig. 4, taken from Ref. 21. In this configuration, the source is the solid metal target, to which a pulsed electrical voltage is applied to create a metal vapor arc. As discussed in Sec. I B, isotope and elemental separations have previously been measured using such devices, although at low throughput and a relatively high energy cost per ion. It is possible to rapidly repeat pulses in this system for higher throughput; for example, a device similar to Fig. 4 has been operated at 5 pulses/s with 10 ms/pulse.[60]

The advantages of this separation mechanism are that the plasma source and separation mechanism are integrated

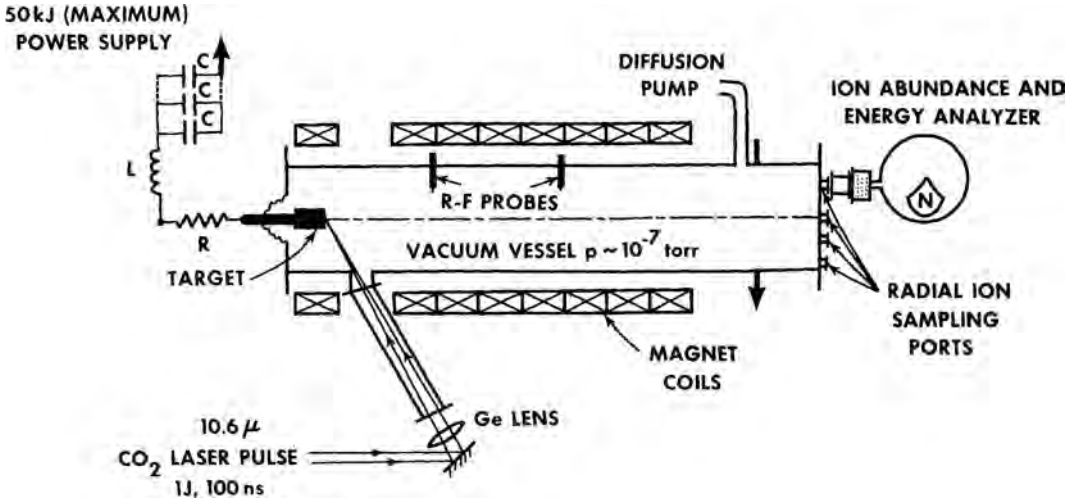

FIG. 4. The original vacuum arc centrifuge for ion separation. The ions are created in a metal vapor arc initiated by a pulsed laser, as shown at the left. The plasma streams down the magnetic field and rotates in the azimuthal direction due to the radial electric field. Heavier ions are forced outward and are deposited at larger radii at the right side. Reprinted with permission from M. Krishnan *et al.*, Phys. Rev. Lett. **46**, 36 (1981). Copyright 1981 the American Physical Society.

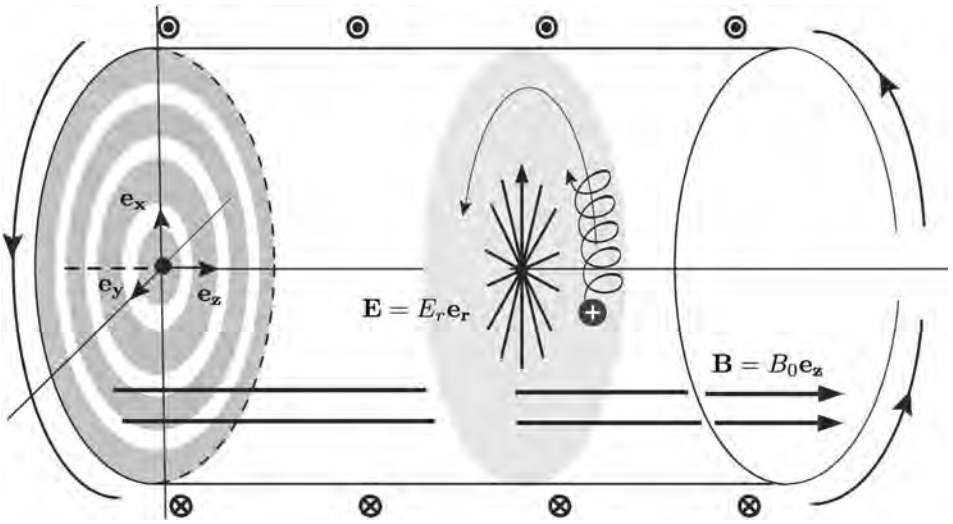

FIG. 5. Configuration for rotating plasma separation in a uniform magnetic field. A radial electric field can be created by a set of annular biased electrodes, as shown at the left. The guiding center orbits drift in the azimuthal direction as shown in the center, with radial excursions which depend on the ion mass. Reprinted with permission from Plasma Phys. Controlled Fusion **60**, 104018 (2018). Copyright 2018 AIP Publishing LLC.

together and that the separation can operate at relatively high collisionality. Two disadvantages of this system are the presence of plasma instabilities,[23,57] which can cause mixing, and its requirement for a conducting solid target, which may not be possible for some input streams. If the energy cost of this method is 70 keV/atom, as estimated in Ref. 23, then the cost would also be too high for the applications mentioned in Sec. I A. A recent review of plasma centrifuges can be found in Ref. 31.

D. Rotating plasma separation (uniform magnetic field)

The centrifugal separation due to rotation can also be created in steady-state uniformly magnetized plasmas by biased annular electrodes, as illustrated schematically in Fig. 5, taken from Ref. 3. The electrodes can create a radial electric field which produces azimuthal rotation at a velocity

$$V_{E\times B} = 10^8\, E(V/cm)/B(Gauss). \tag{4}$$

As discussed in Refs. 3 and 61, the guiding center orbits of ions can produce a radial separation of mass species similar to that in a centrifuge, with either radial vs. axial mass separation (as in the Archimedes filter) or differential radial mass separation in a "double-well" mass filter,[62] depending on the shape and the magnitude of the imposed radial potential and the collisionality. The $E\times B$ rotation velocities needed for significant separation in this regime are apparently fairly high, i.e., $\omega_{E\times B}/\omega_{ci} \geq 0.1$, where $\omega_{E\times B} = V_{E\times B}/a$, where a is the plasma minor radius.

The potential advantages of this method are its capability for allowing external control through biased electrodes and its geometric simplicity. However, the requirement for near-collisionless plasmas will limit the plasma density and throughput, depending on the temperature (see Sec. III F). The rotation speed in partially ionized plasma may also be limited by the "critical ionization velocity" $V_{CIV} \sim (2eI_i/M_i)$, where I_i is the ionization energy of the neutrals.[63] Other potential disadvantages are the difficulty of controlling the radial electric field (see Sec. III G) and the presence of various plasma fluctuations which can cause mixing (see Sec. III H).

E. Rotating plasmas (variable magnetic fields)

The addition of a spatially varying magnetic field to the geometry shown in Fig. 5 can in principal improve the mass separation capability of near-collisionless plasmas, as illustrated in Fig. 6 taken from Ref. 3. For example, a particle at radius r with negative parallel velocity v_{II} in Fig. 6(a) sees a centrifugal potential barrier

$$d\phi = m\omega^2\left(r^2 - r_m{}^2\right)/2. \tag{5}$$

Interestingly, this potential barrier is proportional to the particle mass, and so, for a given parallel energy, there exists a rotation velocity ω for which the light particle can reach r_m while the heavy particle cannot. Assuming a two-ion species plasma in thermal equilibrium, this result can in principle be used to preferentially collect light ions on the small minor radius (left) side.

Another possible configuration adds a magnetic mirror field to the geometry, as shown in Fig. 6(b). In the configuration, $r_m/r > 1$, so that a particle with zero parallel velocity is only confined if

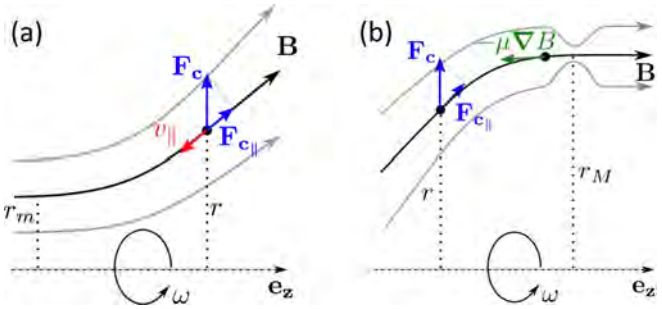

FIG. 6. Configurations for rotating plasma separation with a variable magnetic field. In part (a) is a centrifugal end plug created by an inclined magnetic field, in which light ions preferentially exit at the small radius (left) side. In part (b) is a mirror end plug at a larger minor radius, in which the heavy ions are preferentially lost at the large radius (right) side. Reprinted with permission from Plasma Phys. Controlled Fusion **60**, 104018 (2018). Copyright 2018 AIP Publishing LLC.

$$v_\perp^2 \geqslant [(r_m/r)^2 - 1]\,(B_m/B - 1)^{-1}\, r^2\omega^2 \qquad (6)$$

which creates a loss cone modified by rotation in which the heavy ions are preferentially lost to the large minor radius (right) size.

A combination of these two effects, namely, preferential loss of light ions at a smaller radius in Fig. 6(a) and preferential loss of heavy ions through a magnetic mirror at a large radius in Fig. 6(b), is the basis of the Magnetic Centrifugal Mass Filter (MCMF).[64] In this device, the collisionality has to be large enough for ion-ion pitch angle scattering to scatter ions into the small radius side loss cone, but low enough to limit perpendicular transport. The theoretical mass separation capabilities of this device were further studied through numerical simulations,[65,66] and additional constraints imposed by collisionality were recently clarified.[44] However, no experimental results have yet been obtained on any of these variable magnetic field configurations. An entirely different mechanism for mass separation envisions using rotating magnetic fields.[3,61] Preliminary estimates suggest that rotating plasma separators might satisfy the throughput requirement and be energetically attractive for spent fuel reprocessing applications. This novel approach could be valuable for advanced closed nuclear fuel cycles.[8]

F. Alternative magnetic/electric field geometries

An interesting and extensive set of plasma mass separation designs and experiments using non-uniform magnetic fields have been done at Irkutsk.[40–42] These "Plasma-Optical Mass Separation (POMS)" devices separate ions with ~1 keV using a strong magnetic core ("azimuthator"), taking into account the electric fields from spontaneous charge separation and added thermo-electron emission. The ions are collected at radially or axially separated locations, and successful separation of nitrogen, argon, and krypton has been reported.[42] Further information can be found in a recent review.[31]

An alternative magnetic geometry for ion separation employs an azimuthal magnetic field and a radial electric field, as illustrated in Fig. 7.[45,46] In this concept, a large steady current of ~100 kA is driven in a central conductor which creates the azimuthal magnetic field, which decreases as 1/r from the central conductor. Additional electric fields are formed using ~1 kV electrodes immersed in the plasma (dotted lines), on which the magnetic field lines terminate. The electric potential is assumed to depend logarithmically on the radial position r and to be independent of the axial direction z. Ions are injected either radially or along the z-axis through an annular radial slit. The motion of heavy (A = 238) and light (A = 152) ions is calculated in this geometry, and it is inferred that that separation of spent nuclear fuel with high efficiency can be obtained without significant deposition of ions on the electrodes. However, no experimental results on this mechanism have been obtained so far. Further information can be found in a recent review.[31]

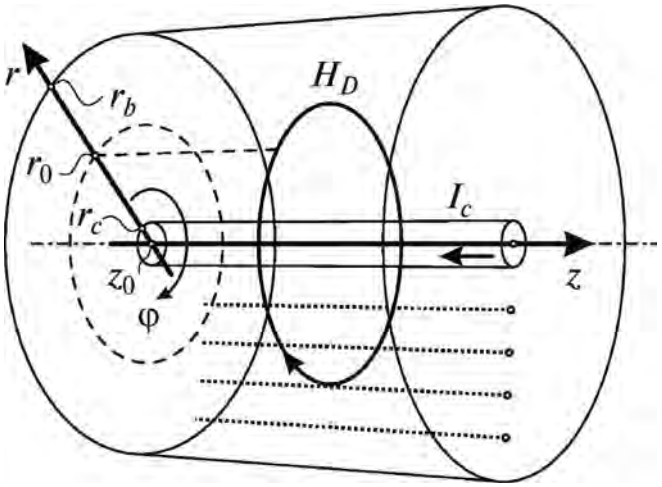

FIG. 7. Azimuthal magnetic field separation. The magnetic field is created by the current I_c in a central conductor, and a radial electric field is created by an array of axial electrodes (dotted lines). Calculations indicate that ion separation can occur without significant ion deposition on the electrodes. Reprinted with permission from A. A. Samokhin *et al.*, Tech. Phys. **61**, 283 (2016). Copyright 2018 Springer Nature.

G. Radial advection

It is often observed that low temperature plasmas in linear magnetic field devices tend to spontaneously rotate in the azimuthal direction, even without externally applied electric fields.[67–69] This rotation is due in part to a radial electric field $E_{rad} \sim 3T_e/a$ caused by the Debye sheath at the axial ends, typically resulting in a velocity of $V_\theta = E_{rad} \times B \leq 1$ km/s at B = 1 kG. If there is a frictional force F_θ on this azimuthal ion rotation which depends on the ion mass, this will cause a radial drift $v_{rad} = F_\theta \times B$ which could be useful for ion mass separation. For ions rotating within a group of neutral atoms at rest, this advection velocity was estimated to be[44]

$$v_{rad} = 9.4 \times 10^{-6} E\,(V/cm)\, n_o(cm^{-3})\, (\alpha_R\, \mu_R)^{1/2}/B^2(Gauss), \qquad (7)$$

where α_R is the relative polarizability of the neutral atom and $\mu_R = M_l M_h/(M_l + M_h)$ is the reduced mass of the colliding species. For example, for E = 1 V/cm, $n_o = 3 \times 10^{13}$ cm^{-3}, $\alpha_R \sim 11$ for $M_l = 40$ (argon), $M_h = 137$ (cesium), and B = 1 kG, it leads to a fairly high $v_{rad} \sim 5 \times 10^3$ cm/s, which depends (weakly) on the ion mass through the reduced mass.

A different radial advection mechanism has been studied recently due to collisionality gradients in a magnetic field with ion diamagnetic flow.[70] The magnitude of the radial drift was found to depend on the ion mass and energy, and a novel scheme was proposed which could produce a substantial ion mass separation at an energy cost of ~1 keV/ion. This theoretical formalism was also used to recover the well-known neoclassical impurity pinch in a tokamak.[71]

Little is known experimentally about the radial advection of ions in linear plasma devices, but outward flow speeds at a surprisingly large $\sim 5 \times 10^4$ cm/s were measured for ArII ions in a helicon device using LIF.[68] Since this ion separation mechanism could occur spontaneously in linear

plasma devices, it is worth investigating in more detail, especially since it may compete with other separation methods. Although radial ion currents due to inertia and viscosity forces in a partially ionized plasmas have been studied theoretically,[72] these effects have not yet been measured experimentally (see Sec. III G).

H. Radial diffusion

Many of the mechanisms discussed above required nearly collisionless ion gyro-orbits or ion drifts in electric and magnetic fields. However, highly collisional plasmas are also interesting for mass separation purposes since they occur at relatively high density, which could produce high throughput, and at relatively low temperature, which reduces the need for auxiliary plasma heating. The collisional motion of ions can be modeled as spatial diffusion in a magnetic field or by the mobility in an electric field (Sec. II I).

When ions are at least partially magnetized, i.e., $\nu_{ii} \leq \Omega_{ci}$, where Ω_{ci} is the ion gyrofrequency and $\nu_{ii} = 2.3 \times 10^{-7}\, n_l\, \lambda\, M_l^{1/2} M_h^{-1} T_i^{-3/2}$ is the ion-ion collision frequency for heavy ions of mass M_h in a (much more dense) background of lighter ions of M_l (both with $Z = 1$), the radial ion-ion collisional diffusion rate is[44]

$$D_\perp \sim {}^1\!/_2 \rho_i^{\,2} \nu_{ii} \sim 1.2 \times 10^{-3} n_l(\mathrm{cm}^{-3}) \lambda\, M_l^{1/2} T_i^{-1/2}(\mathrm{eV}) / B(\mathrm{G})^2 \mathrm{cm}^2/\mathrm{s}, \quad (8)$$

where n_l is the light ion density and λ is the Coulomb logarithm. For $n_l = 10^{13}\,\mathrm{cm}^{-3}$, $M_l = 40$ (argon), $T_i = 10\,\mathrm{eV}$, and $\lambda = 5$, and $B = 1000$ G, the resulting diffusion coefficient is $D_{ii} \sim 10^5\,\mathrm{cm}^2/\mathrm{s}$, which is quite large. However, in this case, the heavy ion diffusion is independent of the heavy ion mass M_h, since its larger gyroradius is offset by its smaller ion collision frequency, and so, there would be little or no ion mass separation. In the opposite limit where $\Omega_{ci} \ll \nu_{ii}$ at high collisionality, the ions would diffuse equally radially and axially, which would produce an isotropic spatial distribution for each species, which would not cause any spatial separation.

Some mass-dependent diffusion might be due to ion-neutral or ion-electron collisions, but these processes are relatively slow. There have been some experimental measurements of "classical" collisional ion diffusion in quiescent linear plasma devices,[73–76] but only in regimes where electrostatic fluctuations are small (see Sec. III H). As far as we know, there have been no measurements of diffusive ion mass separation analogous to gaseous diffusion or diffusive chemical separation.[2] However, the simplicity of this mechanism makes it worth examining in more detail.

I. Ion mobility

Another possible mechanism for ion mass separation is to utilize the drift of ions due to an electric field in a collisional plasma even *without any magnetic field*. The response of collisional ions to a DC electric field E is defined by the mobility μ, where the collisional ion drift speed is $v_d = \mu E$ and[77]

$$\mu = q/(M_i \nu_i), \quad (9)$$

where q is the charge on the ion of mass M_i and ν_i is the total ion collision frequency with all species. The corresponding flux of this ion species with a density n_i in the direction of the electric field E is

$$\Gamma = n_i v_d = \mu\, n_i E = q\, n_i E/(M_i \nu_i). \quad (10)$$

For ions colliding with neutrals, the ion-neutral collision frequency is approximately independent of ion velocity in the low-temperature limit ($T_i < 3$ eV), with $\nu_{io} = K\, n_o$, where K depends on the neutral species and ion mass.[44,77] In this case, the flux of ions along the direction of the electric field will depend inversely on the ion mass, which is a fairly strong separation mechanism. For heavy ions colliding with light ions, the collision frequency depends inversely not only on the heavy ion mass M_i but also on the light ion mass $M_j^{1/2}$.[44] In general, the mobility of heavy ions tends to be lower than that of light ions due to their lower thermal speed.

The throughput of such a scheme will depend (among other things) on the average ion drift speed, which depends on the ion energy gain in the electric field over a collision mean free path L_{coll}, or roughly

$$v_d/v_i \sim (E\, L_{coll}/T_i)^{1/2}. \quad (11)$$

For a helicon plasma like that in PMFX[43] with $n_i \sim 10^{13}\,\mathrm{cm}^{-3}$ and $T_i \sim 1$ eV, the ion-ion collision length for a heavy ion with $M_h = 84$ (krypton) on a background of light ions with $M_l = 40$ (argon) is roughly $L_{coll} \sim 0.1$ cm, and so, an electric field of $E = 1$ V/cm will produce a drift speed of roughly $v_d \sim 0.3 v_i$, which seems to be consistent with a reasonably high throughput.

There are difficulties in implementing this mechanism in a high throughput plasma mass separator. First, the directed ion flux due to the mobility will have to compete with the random motion due to thermal ion collisional diffusion, which will set a minimum level of the electric field required for separation. Second, most of the electric field will be shielded from the plasma by a Debye sheath of $\lambda_d \ll 1$ mm although the electric field of the larger pre-sheath region has been seen to cause mobility-limited ion flow.[78] There are several existing ion mobility mass spectrometry (IMMS) techniques to analyze the mass spectrum of organic compounds, based on (un-neutralized) ion drift motion in a buffer gas in static or time-dependent electric fields, as described in reviews such as Refs. 79 and 80. For example, there are 50 000 handheld analytical mass spectrometers of this type being used for chemical weapon and explosive monitoring. Thus, it might be interesting to explore this mechanism further in a neutralized plasma.

There are also some interesting experiments on isotope separation in high pressure, high current density DC discharge plasmas in a thin capillary tube.[81] Experiments in neon and krypton show modest enrichment of heavy isotopes near the cathode region in steady-state discharges, i.e.,

opposite to the direction expected from the mobility argument above. Three theoretical mechanisms were considered: radial separation due to thermal diffusion, "isotopic cataphoresis" due to differential ion loss to the wall, and differential friction of ions onto neutrals called the "ion wind." The latter was considered the most probable within the context of the experiments in Ref. 81. This appears to be a slow process and so is not likely to be useful for high throughput separation.

J. Ionization energy

Another simple concept for ion mass separation would be to control the electron temperature within the plasma to differentially ionize atomic or molecular species. The electron temperature can in principle be controlled by localized heating, e.g., using electron beams or ECRH resonance with a magnetic field, and an applied electric field can be used to collect the ions even without a magnetic field (Sec. II I). Such a differential ionization process may also be relevant for understanding the boundary region between plasmas and neutral gas[82] or in the spontaneous chemical separation of astrophysical plasmas.[83]

For example, the ionization energy of cesium is the 2nd lowest of all elements (3.9 eV),[84] and so, its ionization threshold might be useful to separate the radioactive isotope Cs^{137} from other species, even if Cs was in molecular form. However, since the cross-sections for ionization of atoms and molecules are the slowly varying functions of electron energy, and even more slowly varying functions of the electron temperature, it would be difficult in general to obtain a sharp mass separation with this mechanism. The ionization cross-sections as a function of electron energy for many of the oxides present in spent nuclear fuel are discussed in Ref. 6 and references therein. A typical electron energy of $E \geq 5$ eV is required to ionize oxide molecules such as UO_2, Nd_2O_3, and ZrO_2.

K. Transit time separation

Small samples are routinely analyzed and separated by mass using high resolution TOFMS (time-of-flight-mass spectroscopy), where ions are created with pulsed sources and detected with microchannel plates.[12,85] Spatial separation has also been obtained using distance-of-flight spectroscopy with a modified instrument and phosphor plate detection.[86] However, these devices have only a microscopic throughput due to space charge limits.

It might be possible to extend this simple principle to high throughput mass separation using a pulsed plasma source and a rotating collector plate synchronized with the source, as illustrated schematically in Fig. 8. For this purpose, the ions should have a fairly well defined energy, perhaps obtained using a pulsed sputtering target with ion energy control grids. If the ion energy was 10 eV, the difference in transit time for ions of $A = 40$ and $A = 250$ over a drift length of 10 meters would be ~3 ms, which would produce a spatial separation of ~3 cm on a collection plate moving at ~10 m/s. This is a small spatial separation, but not much different from that used in the original calutron devices (Sec. I B).

In a device of this type, the ions could be guided along the drift tube by an axial magnetic field, but the collisionality must be low enough to avoid significant scattering. The ions need to be accelerated to a near-constant energy, perhaps with electrostatic grids at either or both ends. Fixed radial slits at the far end would allow spatial dispersion onto the rotating collector plate. An advantage of this geometry is that a rotating collector plate could be mechanically segmented and the collected material could be readily segregated when the plate is removed. Difficulties include the need for a near-monoenergetic low energy ion beam, the inefficiency due to the slit transmission and pulsed duty cycle, and the mechanics of rapid rotary motion in a vacuum system.

III. GENERIC PHYSICS ISSUES

This section describes some generic physics issues which need to be considered in the design of plasma-based mass separation devices. Here, the composition of the material to be separated is not specified, in order to incorporate the various applications of Table I and others unforeseen. Generic technology issues are discussed in Sec. IV.

A. Charge state

In order to efficiently separate ions using the mechanisms of Sec. II, it is highly desirable to maintain a single ion charge state of $Z = +1$ for all species since all the separation mechanisms depend on the ion charge/mass ratio. The average atomic ion charge $\langle Z \rangle$ generally increases with the electron temperature and (to a lesser extent) with electron density; however, these dependences vary significantly with each species, and so, detailed calculations are needed.

For example, the calculated average ion charge state for sodium ($Z = 11$) and gold ($Z = 79$) vs. electron temperature

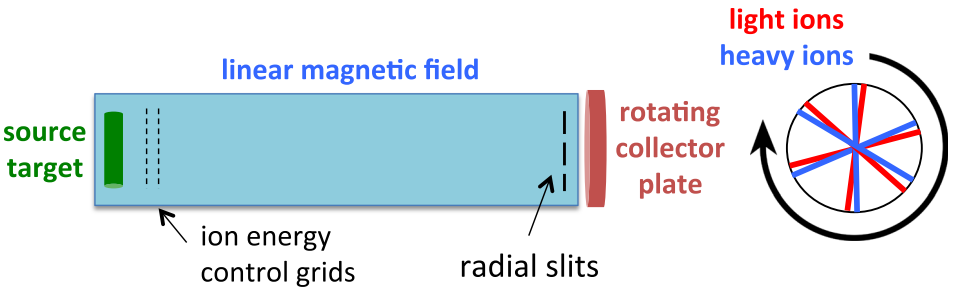

FIG. 8. Concept of transit time ion separation. The pulsed plasma source emits ions which are accelerated to a fixed energy by the control and become separated along the magnetic field due to their different velocities. A rotating wheel with slits is used to deposit ions with different masses at different angles.

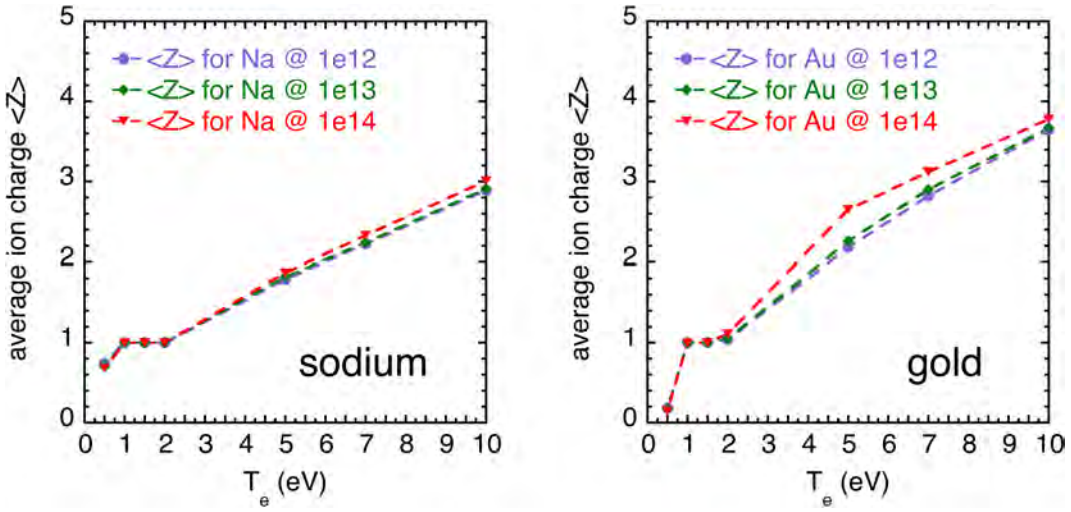

FIG. 9. Average ion charge state vs. electron temperature calculations from the FLYCHK atomic physics code.[87] At the left are the results for sodium (M = 22), and at the right are the results for gold (M = 197). For both cases, the average charge state is ⟨Z⟩=1 only in the range of T_e = 1–2 eV.

is shown in Fig. 9 for three assumed electron densities, based on the IAEA atomic physics code FYLCHK.[87] Sodium is one of the most common low mass elements in the Hanford nuclear waste (see Sec. I B), and gold is the highest Z in this database. Similar databases can be found elsewhere,[88,89] but all of them are based on simplified atomic physics models (e.g., assuming equilibrium) and not on direct experimental measurements. Note that FLYCHK is optimized for highly ionized states, and so, these results for low ionized states are not expected to be highly accurate and should be checked with the best available codes for each species.

Based on Fig. 9, the desirable average charge state of ⟨Z⟩=1 for both sodium and gold occurs at $T_e \sim 1$–2 eV, independent of electron density in the range of $n_e = 10^{12}$–10^{14} cm^{-3}. Above this temperature, the average charge state increases to ⟨Z⟩ = 2 at $T_e \sim 5$ eV, at which point most ion separation mechanisms will be seriously compromised due to the change in the charge/mass ratio. Thus, a requirement of Z = 1 most likely constrains the device operation to $T_e \sim 1$–2 eV. This constraint was previously noted within the context of the TRW uranium isotope separation process,[90] which was performed at $T_e \sim 1$ eV.

A related issue is the expected variation in the charge state distribution with the atomic species, even at the optimum electron temperature. Two examples are shown in Fig. 10: at the left is cesium, which has a low ionization potential of 3.9 eV, and at the right is argon, which has a relatively high ionization potential of 15.8 eV. Both are taken from the same FLYCHK code used for Fig. 9 (Ref. 87) for $n_e = 10^{13}$ cm^{-3}. At $T_e = 1$ eV, the dominant charge state for cesium is "1," while that for argon is "0" (i.e., neutral); at $T_e = 2$ eV, the dominant charge state for cesium is "2," while that for argon is "1." Thus, it would be very difficult to maintain a dominant charge of +1 for both species in this temperature range and even more difficult given the expected spatial variations of temperature and density within the plasma. Detailed calculations of the charge state distributions are available for vacuum arc plasmas,[91] which show multiple charge states for most metallic elements in such arcs.

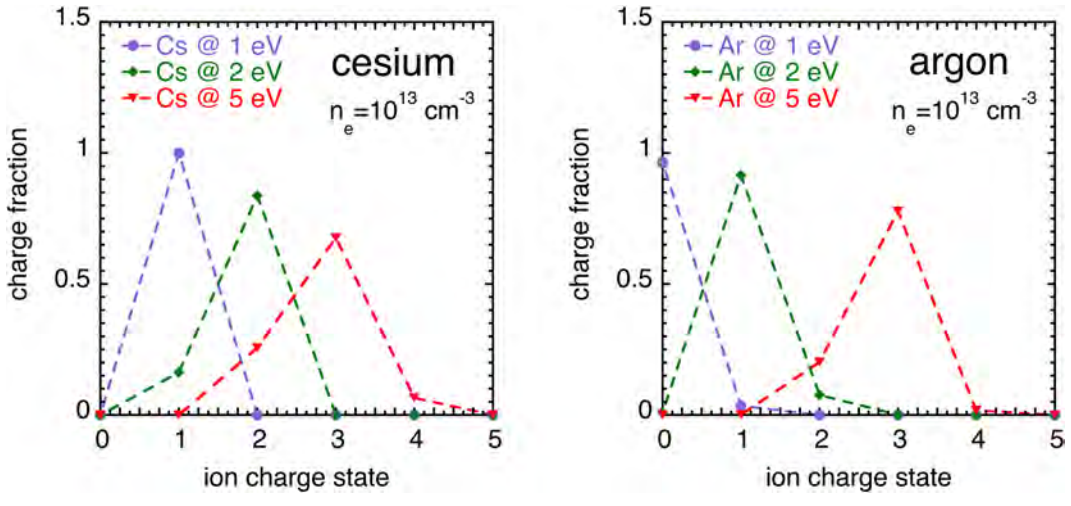

FIG. 10. Calculated charge state distribution for cesium (left) and argon (right) from the FLYCHK atomic physics code.[87] The charge state distributions at a fixed temperature in the range of T_e = 1–2 eV are different due to the much lower ionization potentials for cesium (3.9 eV) compared to argon (15.8 eV).

B. Neutrals

Neutral atoms will not be separated by any of the mechanisms of Sec. II and so will tend to reduce the separation and throughput with respect to idealized calculations with a fully ionized plasma. As discussed in Sec. III A, it is likely that there will be a significant neutral population for those species with a high ionization potential (such as argon) and in spatial regions where the electron temperature is low (such as near the walls). The neutral density in the separation experiments of Table II was not measured directly, but it is likely that the volume-averaged neutral density will be $n_o \sim 10^{14}\,cm^{-3}$ (see Table III), comparable to or higher that the volume-averaged ion and electron density.

The transport rate of neutrals through a plasma mass separation device will depend on the neutral speed, the neutral collisionality, and the neutral pumping process. If the neutrals were at room temperature, their transport through the system would be relatively slow compared to the ions, and their throughput may be relatively small. However, it is possible that ion-neutral collisions and charge exchange will heat the neutrals to near the ion temperature, in which case the local flux of neutral atoms could be larger than the ion flux. The quantitative effect on separation will then depend on the collection or exhaust mechanism for ions vs. neutrals. If the ions were collected in a way that excluded neutrals, e.g., using ion deposition onto a charged plate, then the neutrals might be recycled back into the main separation chamber without lowering the separation efficiency. However, if the ions were first neutralized and then exhausted by a vacuum pump, then the background neutrals could seriously dilute the separation efficiency. The results will also depend on the mechanisms by which ions and neutrals interact with surfaces, which itself can be quite complicated.

A potentially useful option in a plasma mass separation device is to intentionally add an inert neutral "buffer gas" like argon to stabilize the performance of the plasma with respect to variations in the input feed stream. Argon is often used to create RF plasmas in basic plasma experiments and processing plasmas.[67–69,77] An inert buffer gas might have a relatively high neutral density but would recycle from the chamber walls and could be pumped out of the system and returned to the main chamber for steady-state plasma operation.

Quantitative modeling of neutral transport in plasmas is a formidable challenge due to the interaction of atomic physics, surface physics, and plasma transport effects. Neutrals in low temperature edge plasmas in magnetic fusion are modeled using coupled plasma fluid and kinetic neutral codes,[92] but the difficulty of measuring the local neutral density limits their experimental validation.[93] It is likely that new codes will have to be written to treat neutral transport along with the other generic physics issues in mass separation devices (see Sec. V C).

C. Molecules

The two Sections III A and III B assumed that all species were in simple atomic form. However, many of the raw materials to be separated (for example, nuclear waste) will also consist of molecules such as metallic oxides and nitrides. Thus, at low electron temperatures, there could be significant molecular ion components in the plasma in addition to atomic ion species. The subject of molecular ionization and dissociation is treated extensively in the literature of mass spectroscopy,[11,12] where it is desirable to ionize molecules without breaking them apart, and in plasma chemistry and plasma processing, where molecular reactions and plasma-surface interactions are dominant.[77,98]

The main molecular issues in plasma mass separation are to determine the expected charge state, effective mass, and relative density of molecules at the electron temperatures of interest. Although all the mechanisms in Sec. II will apply to (positive) molecular ions as well as to atomic ions, the presence of molecules with a varying mass for each species will make it more difficult to cleanly separate low mass atoms from high mass atoms in a plasma. In general, the behavior of even simple molecules in plasmas is extremely complicated, involving many distinct processes such as electron impact ionization and dissociation, recombination, electron attachment and detachment for negative ions, metastable states, charge exchange reactions, and vibrational and rotational excitations. For example, in Ref. 77, there is a table of 33 selected second order reaction rate constants for oxygen discharges, including O, O_2, O_3, O^+, O^-, O_2^+, O_2^-, and O_3 components and their metastable states, with cross-sections which vary greatly with electron energy over the range of ~0.1–10 eV. Note that negative ions (which commonly form in low temperature plasmas) will behave very differently from positive ion atoms or molecules in a separation device.

The ionization energy of many molecules is tabulated in the NIST Chemistry WebBook,[95,96] Almost no molecules have an ionization energy below that of a cesium atom (3.9 eV) or above that of a helium atom (24.6 eV), and so, the range of molecular ionization energies largely overlaps that of single atom species. For example, the ionization energy of a Na atom is 5.1 eV, a NaCl molecule is 8.9 eV, a U atom is 6.2 eV, and a UCl_4 molecule is 9.2 eV. Thus, the average ionization state of the molecules in a plasma device should be roughly similar to that of the constituent atoms, and so, if the plasma is optimized to have $\langle Z \rangle = 1$ for atoms at $T_e = 1$–2 eV, the ionization state of the molecules in this plasma should be roughly similar.

The concentration of molecular ions in a nuclear waste plasma is difficult to estimate from first principles but will depend on the ionization source technique (see Sec. IV A) and the rate of molecular dissociation at the plasma electron temperature and density within the separation volume. The energy required for breaking molecular bonds is typically in the range of ~1–10 eV, e.g., 1.5 eV for an O-O bond and 8 eV for NaCl, i.e., overlapping with the range of ionization of these molecules.[97] Evaporation, ionization, and dissociation of atoms and molecules in spent nuclear fuel are extensively tabulated in Ref. 6. In general, molecular dissociation in a plasma is a complex process which depends on the excitation states of the bound electrons and the electron energy distribution.[94] Molecular effects will need to be studied with dedicated plasma simulation codes such as used for plasma processing[77] and plasma chemistry.[94,98]

D. Charge exchange and recombination

The ion separation mechanisms discussed in Sec. II will be compromised if the ions inside the plasma turn into neutrals before they can be separated. When an ion picks up an electron from a neutral atom or molecule, the process is known as charge exchange (or a charge transfer reaction). When an ion and an electron combine to form a neutral atom or molecule, it is known as recombination.

The distance an ion will travel before a charge exchange reaction will be

$$L_{cx} = 1/(n_o \sigma_{cx}), \tag{12}$$

where n_o is the neutral atom density for any species of interest and σ_{cx} is the charge exchange cross-section for that specific ion-neutral pair, which depends on their relative velocity and electronic states. In general, there can be both resonant charge exchange reactions between atoms and ions of the same species, and non-resonant charges exchange reactions between ions and atoms of different species.

In the context of plasma mass separation, the charge exchange processes of interest are mainly those between heavy ions and light neutral atoms (or molecules) and *vice versa*. For example, if a heavy ion is being separated using an electric field (Sec. II I), its transport and extraction will be inhibited when L_{cx} is less than the system size. Charge exchange between a heavy ion and a heavy neutral atom will also be important if the separation mechanism depends on the ion energy, which can be changed by this reaction.

The cross-sections for resonant charge exchange of noble gas ions were measured to increase monotonically with decreasing energy up to $\sigma_{cx} \sim 3 \times 10^{-15}$ cm^2 at $T_i = 4$ eV for He, Ne, and Ar.[77] Several measurements and modeling of argon resonant charge-transfer cross-sections also showed $\sigma_{cx} \sim 3$–4×10^{-15} cm^2 over the range of $T_i = 1$–10 eV.[99] For a cross-section of $\sigma_{cx} \sim 3 \times 10^{-15}$ cm^2 and $n_o = 10^{14}$ cm^{-3}, the resulting charge exchange distance is roughly $L_{cx} \sim 3$ cm, which is smaller than a typical plasma size, and so, charge exchange would be important in the discharge modeling.

The resonant charge exchange cross-sections for other monatomic gases in the range of $v_i \sim 10^5$–10^7 cm/s have been approximated analytically. These cross-sections generally increase with decreasing ionization potential and decreasing particle velocity; for example, the calculated cesium resonant cross-section at $T_i = 4$ eV is large $\sim 3 \times 10^{-14}$ cm^2, and the measured value is apparently even higher.[100] This implies a very small charge exchange distance of $L_{cx} \sim 0.3$ cm at a neutral cesium density of 10^{14} cm^{-3}, which would make this a dominant process. Many other charge transfer cross-sections can be found in the IAEA Aladdin database[101] and some in the Atomic Data and Nuclear Data Tables (ADNDT)[102] and the Plasma Data Exchange Project (PDEP).[103] For example, the charge transfer cross-section between Na^+ and O^- ions is $\sigma_{cx} \sim 30 \times 10^{-15}$ cm^2 at a relative velocity of 4×10^5 cm/s,[104] which would again be a dominant process.

Recombination is a process in which a positive ion combines with a free electron (or negative ion) and transforms into a neutral atom. For example, the electron-ion recombination rate coefficient for $e + N_2^+ = N + N$ for room temperature ions with $T_e = 1$ eV is $k = 3 \times 10^{-8}$ cm^3/s;[94] thus, N_2^+ has a lifetime of only $\sim 3\,\mu$s at $n_e = 10^{13}$ cm^{-3}, and so, this could be an important process in a nuclear waste plasma. The analysis of charge exchange and recombination would probably require data mining for cross-sections and detailed computational simulation (see Sec. V C).

E. Droplets, dust, and nanoparticles

Most attempts to convert a solid input stream into an atomic or molecular plasma will be incomplete, resulting in macroscopic droplets ($\sim 100\,\mu$m), dust ($\sim 1\,\mu$m), and/or nanoparticles (~ 10 nm) in the plasma. For example, liquid droplets or macro-particles are normally evaporated from metallic cathodes in vacuum arc plasmas (see Sec. II C), and deliberate dust injection might be used to create the plasma source (see Sec. V A). The effects of these large particles on a separation device will depend on their species composition, charge/mass ratio, number density within the plasma, and flow speed.

Typical surface charges on a large droplet $\geq 10\,\mu$m will be negligible with respect to their mass, with charge/atom ratios of roughly $< 10^{-8}$. These droplets will act essentially as neutral particles and will not be separated in a plasma mass separation device, as noted in vacuum arc devices.[38] Smaller macro-particles of $\leq 10\,\mu$m in pulsed vacuum arcs can be deflected by electric and magnetic fields,[105] but this is not helpful unless they have a mass-separated charge distribution. A method of vacuum arc plasma separation of macro-particles has been developed in Israel which directly converts metallic droplets into metal plasma without using complicated centrifugal or magnetic filters.[106–108] This method uses a metallic cathode and a non-consumable refractory anode which is heated during operation of the arc. This could be a useful plasma source for mass separation of metallic materials such as spent nuclear fuel.

Typical charges on micron-sized dust in steady-state low temperature laboratory "dusty plasmas" are $\sim 10^3$–10^4 electrons, with typical dust particle densities of $\sim 10^4$ cm^{-3} and dust flow velocities ≤ 10 cm/s.[109–111] Thus, the average charge per atom (e.g., for $1\,\mu$m aluminum dust) is $\sim 10^{-6}$ e$^-$/atom. Even though charged dust in plasmas can respond to electric and magnetic fields, the mechanisms of Sec. II will not work with atoms and dust at the same time. For dust particles to have a negligible effect on the separation process, their number density needs to be $< 10^2$ cm^{-3}, which is considerably lower than the dust density in a typical dusty plasma experiment.

Smaller nanoparticles or "clusters" of ~ 1–10 nm in size with $\sim 10^5$–10^8 atoms are sometimes formed in low temperature processing plasmas[94] and have also been studied in the context of femtosecond laser-plasma interactions.[112,113] It is not clear whether or how such clusters would be formed in a complicated plasma separation environment, or if so, whether their composition would segregate high mass from low mass atoms. However, since their charge/atom ratio would still be much less than singly charged atoms or molecules, they would not be separated in the same way. The conclusion from this

section is that the plasma source and plasma heating systems should be designed to minimize particles larger than molecules. This will probably require diagnostics of the particle size distribution in these plasmas, e.g., using lasers.[114]

F. Collisions

The transport and separation of ions through a plasma mass separator will be modified by Coulomb collisions with other ions, electrons, and neutrals. These collisions will generally impede the flow of ions through the system, but differences in the collision rate among ions might also be useful in the separation process. For simplicity, in this section, we consider collisional effects only for singly charged atoms, but similar collisional effects will occur with multiply charged atoms and molecules and with neutrals.

A theoretical analysis of collisional effects in axial-collection plasma mass filters has been published recently,[44] focusing mainly on cylindrical linear magnetic devices like the PMFX.[43] This model included ion-ion and ion-neutral collisions and ion gyroradius motion and calculates radial and parallel transport timescales for low mass and high mass ions due to collisional diffusion and advection. The ion-ion collision frequency ν_{ii} for 90° scattering of minority heavy mass ions M_h (amu) on majority low mass ions M_l (amu) at a common ion temperature T_i (eV) and density n (cm^{-3}) is

$$\nu_{ii} = 2.3 \times 10^{-7} n_l \lambda M_l^{1/2} M_h^{-1} T_i^{-3/2}, \quad (13)$$

which can be used to determine the parallel mean free path for ion-ion collisions $L_{mfp} = v_i/\nu_{ii}$ and the parallel ion diffusion rate $D_{||}$ for heavy ions

$$D_{||} = (3/2) v_i^2/\nu_{ii} \quad (14)$$

and so, the parallel collisional confinement time of a collisional ion along a magnetic field of length $L_{||}$ is

$$\tau_{||D} = (L_{||}/2)^2/D_{||} = L_{||}^2 \nu_{ii}/6v_i = 4.0 \times 10^{-20} n_l \lambda L_{||}^2 M_h^{1/2} T_i^{-5/2}. \quad (15)$$

For the basic plasma parameters in Table II, the heavy ion has $L_{mfp} \sim 10$ cm, which is near the heavy ion gyroradius for $M_h = 80$ at B = 0.2 T. The heavy ion confinement time from Eq. (15) is $\tau_{||D} = 0.6$ msec, which is longer than the collisionless ion confinement time of $\tau_{||} \sim (L_{||}/2)/v_i \sim 0.2$ ms. Thus, the parallel throughput would be reduced due to ion-ion collisions. The effects of ion-neutral collisions were also considered, but these tend to be lower even at an assumed $n_o = 10 n_i$.[44]

The conclusion from this section is that collisional effects can be important for the plasma mass separation, especially at high densities and low ion temperatures. Ion collisions will tend to mix the spatial separation driven by the mechanisms in Sec. II and also limit the throughput (see Sec. III K). The basic atomic cross-sections for most simple collisions are available in textbooks[77,94] or online databases.[115] Other collisional processes may also need to be considered, such as inelastic (energy absorbing) collisions with molecules and collisions with dust or other particles.

G. Electric fields and rotation

Some of the ion mass separation mechanisms in Sec. II involve the imposition of DC electric fields to the plasma, either to differentially transport ions or to control plasma rotation through E × B drifts. The degree to which an electric field in a plasma penetrates along or across a magnetic field is difficult to calculate theoretically, and so, understanding and controlling electric fields and rotation in these plasmas can be a major issue in plasma mass separation. For example, the effects of electrodes on the radial potential profiles in linear RF devices such as PMFX,[43] CSDX,[69] and HelCat[116] were not well understood although the plasma E × B rotation in these devices and in plasma centrifuges[23,25] is apparently consistent with the measured potential profiles.

The main reason for this difficulty is the complicated physics of cross-field electrical conductivity in low temperature magnetized plasmas, which depends on the ion-ion and ion-neutral friction (including charge exchange), which determines the perpendicular ion viscosity.[72] The difficulty is further increased by the complexities of sheath physics, even in an un-magnetized plasma,[78] and by the cross-field conductivity and/or plasma flows which could be created by fluctuations (see Sec. III H). Since the electrostatic potential distribution is determined by both the radial and parallel currents, the electric fields will depend on the full 3d geometry of the device, making experimental validation of theoretical models difficult.[117] Any small conducting path can "short out" the attempt to impose a desired electric field.

Thus, the self-consistent electric fields within a plasma mass separation device cannot be calculated from first principles without knowing the plasma density and temperature profiles, the neutral density profile, and the plasma instabilities, thus coupling together many of the physics issues of this section. A similar complex situation exists in magnetic fusion plasmas, especially in the edge region where neutrals and radial electric fields can also be important.[118] Sophisticated computational codes such as BOUT++[119] and XGC1[120] are being developed to handle such problems.

H. Plasma fluctuations

The mass separation for most of the mechanisms in Sec. II can also be compromised by spatial mixing associated with plasma fluctuations, which were not incorporated into any of those models. In general, the longer an ion is confined within the plasma volume, the more likely the plasma fluctuations will affect its spatial separation. The physics of plasma fluctuations is nonlinear and sensitive to the details of plasma parameters, plasma flows, electric fields, and boundary conditions. Plasma fluctuations have been seen in many previous experiments on ion mass separation, including the arc plasmas used in uranium isotope separation,[121] which motivated the Bohm diffusion coefficient

$$D_B \sim 6 \times 10^6 T_e(eV)/B\,(G)\ cm^2/s. \quad (16)$$

Even though there is no clear physical basis for this formula, it is sometimes used as a benchmark to estimate the relative effects of turbulent transport vs. collisions.[44]

Although plasma fluctuations were observed in plasma arc centrifuges[23,30] and in the PMFX experiment,[43] there has not been a direct measurement of their effect on ion diffusion or spatial mixing in these separation experiments. However, it is clear that linear helicon devices like CSDX,[69] HelCat,[116] and HELIX[122] can become very unstable and turbulent at $B \geq 1$ kG, with potential fluctuations of $e\phi/Te \geq 1$ which can extend over much of the radial profile. For example, if these fluctuations created an azimuthal electric field of $E \sim 1$ V/cm at $B = 1$ kG, the resulting radial $E \times B$ drift is $V_r \sim 10^5$ cm/s, which is comparable to the heavy ion speed at $T_i \sim 1$–10 eV. Such a large convective $E \times B$ flow would cause significant displacement of ions over a timescale of $\tau_{turb} \sim a/V_r \sim 50\,\mu$s, which is significantly lower than the estimated Bohm diffusion time of $\tau_B \sim 1$ ms for this system.

Plasma instabilities are generically categorized as either electrostatic drift wave or magnetic (MHD) instabilities. The former are commonly seen in linear current-free plasma devices, while the latter are often seen in high-current arc plasmas. Electrostatic instabilities tend to move all ion species together at the $E \times B$ drift speed, independent of their charge/mass ratio, and so, they would not directly cause ion mass separation; however, in MHD instabilities, the ions move along the perturbed magnetic fields at their thermal speed, which does depend on the ion mass. The ion transport rate for these instabilities depends on many factors such as the frequency spectrum, the size scale spectrum, and the fluctuation levels, none of which can easily be predicted. Other types of plasma instabilities might occur at the ion gyrofrequency or bounce frequency in mirror devices, and wave-induced ion transport due to RF electric fields in the plasma might also be significant. The stabilizing/destabilizing role of rotation in magnetized plasma experiments, in particular for separation, is discussed in a recent paper.[123]

I. Atomic radiation

Turning now to the issue of the energy requirements for plasma mass separation, an important part of the energy balance is the atomic (line) radiation from the plasma, which generally increases linearly with electron density and also with the atomic number (or ion mass) at a fixed T_e. We assume that the plasma is optically thin to this radiation (which is mainly in the visible and UV regions) and estimate the radiated power to the wall from theoretical atomic physics codes. These code results should only be considered as rough guidelines since they make many simplified approximations in the atomic physics models.[87–89]

Radiated power results from the FLYCHK atomic physics database[87] are illustrated in Fig. 11 for sodium (common in the Hanford waste) and for gold (the highest atomic number in this database). The calculated radiated power for a 100% sodium plasma at $n_e = 10^{13}\,cm^{-3}$ is $P_{rad} \sim 10^{-4}\,W/cm^3$ at $T_e = 2$ eV, which is small compared to the typical RF heating power of $P_{rad} \sim 10^{-2}\,W/cm^3$ in existing devices.[43] However, the calculated radiation power for gold at $n_e = 10^{13}\,cm^{-3}$ at $T_e = 2$ eV is $P_{rad} \sim 500\,W/cm^3$, which is $\sim 5 \times 10^6$ times higher than that for sodium at this temperature. Thus, the calculated radiated power for a plasma with only 1% gold at $n_e = 10^{13}\,cm^{-3}$ and $T_e = 2$ eV is $P_{rad} \sim 5\,W/cm^3$, which is very high compared to the usual RF heating. This large radiated power can presumably be expected for all high mass ions such as uranium although for quantitative results, the calculations should be re-done using codes which are more appropriate for low temperatures and low ion charge states.

It would be useful to know the total energy radiated per ion in order to estimate the energy costs for plasma mass separation. The total radiated power depends on both the radiation rate and the confinement time of the ion in the system. For example, if a gold ion radiated at $P_{rad} \sim 500\,W/cm^3$ at $T_e = 2$ eV and $n_e = 10^{13}\,cm^{-3}$ and was confined for 0.6 ms (see Sec. III F), the total radiated power would be ~200 keV/ion, which is much higher than the ionization energy; however, the corresponding result for sodium is <1 eV. Since the ion confinement time is highly variable depending on the specific separation mechanism, the radiation energy cost per atom cannot be calculated without further information about the history of the atoms in the system. Further discussion of the required modeling is given in Sec. V C.

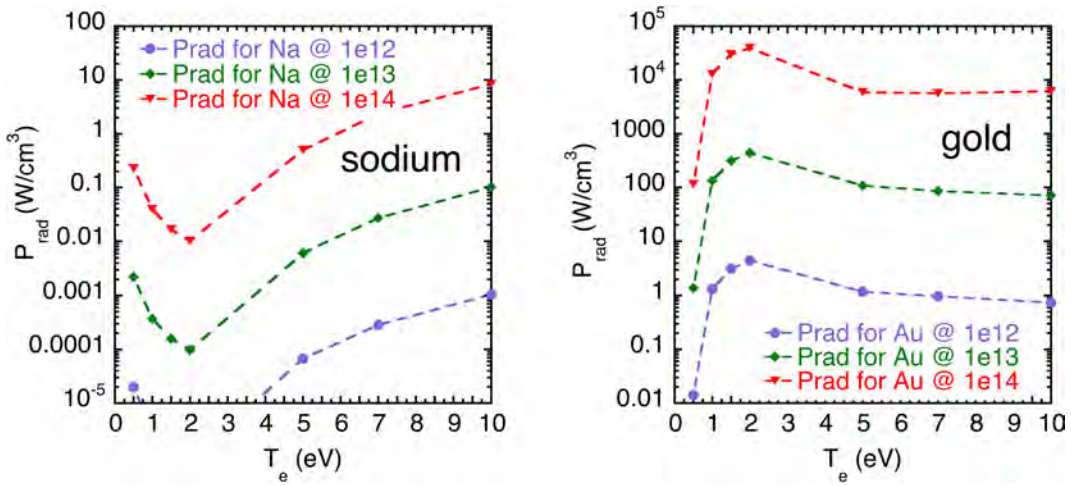

FIG. 11. Theoretical calculations of the radiated power for sodium (left) and gold (right) for three densities as a function of T_e from the FLYCHK atomic physics code (taken from Ref. 87). The radiated power expected for sodium at $T_e = 2$ eV and $n_e = 10^{13}\,cm^{-3}$ is $P_{rad} \sim 10^{-4}\,W/cm^3$, but for these conditions, for a 1% density of gold, it is $\sim 5\,W/cm^3$.

J. Plasma energy loss

The loss of plasma energy to the chamber walls will also affect the electrical cost of plasma separation. The plasma power loss rate to an insulating wall can be written in a simplified form as[124]

$$P_{loss}\left(W/cm^2\right) \sim \gamma T_e \Gamma\,(\text{ions/cm}^2\text{-sec}), \tag{17}$$

where γ is the total heat transmission coefficient and Γ is the flux to the wall. For $T_i \sim T_e$, the usual result is $\gamma \sim 7$–8,[124] comprising ~5–6 for electrons and ~2–3 for ions, since the electrostatic sheath accelerates ions and decelerates electrons across a potential of $\sim 3T_e$ to keep the net current to the wall zero. For $T_i/T_e = 5$, the heat transmission coefficient increases to $\gamma \sim 15$. In this model, the total energy cost per ion at $T_e \sim 2\,eV$ and $T_i = 10\,eV$ would thus be ~30 eV, which is a few times the ionization potential for most atoms. Of course, the energy loss per ion would be larger for very high energy ions such as those accelerated by ICRH, but these may be a relatively small fraction of the ions. Further complications arise when the wall is conducting or biased or when there is significant secondary electron emission from the wall.[124]

Perhaps a bigger issue is the heat loading on the walls, which could require active cooling if the wall temperature becomes too high. Assuming an ion wall flux of $\Gamma \sim 1/2\ n_i v_i$ for $n = 10^{13}\,cm^{-3}$, $M_i = 40$, $T_i = 10\,eV$, and $T_e \sim 2\,eV$, the wall heating from Eq. (17) will be $\sim 10\,W/cm^2$, which is moderately high but not excessive. However, if internal biased electrodes are incorporated in the design, the heat flux onto them could be much larger, and they would be more difficult to actively cool (see Sec. IV B).

K. Ion throughput

The goal of a plasma mass separation is to produce a usefully high throughput of ions which are physically separated according to their mass range. As discussed in Sec. I A, a useful throughput can be anywhere from ~0.01–100 g/s, depending on the application (see Table I). The maximum possible (collisionless) ion throughput for a plasma with exhaust area A (cm^2) is the ion flux to the wall

$$\Gamma(g/s) \sim {}^1\!/_2\, n_i v_i A \left(M/6 \times 10^{23}\right). \tag{18}$$

Assuming $T_i = 10\,eV$, $M = 40$ amu, $n_i \sim 10^{13}\,cm^{-3}$, and an exhaust area of $\sim 10^4\ cm^2$, this is equivalent to a throughput of ~1–2 g/s, which is not far from the desired throughput range. Of course, this assumes that the plasma separation physics, the ion source generation, and the waste exhaust process are all operating at this throughput level (see Secs. IV A and IV C for the latter two issues).

More realistic collisional calculations of the ion throughput for one specific MCMF (magnetic centrifugal mass filter) configuration have been made using simplified analytic estimates and a Monte Carlo ion orbit simulation model for an argon/krypton mixture.[44] For most cases, the plasma is collisional (see Sec. III F), and so, the parallel ion transport is diffusive; the theoretical maximum throughput does *not* increase with density as in Eq. (18) since the ion mean free path will also decrease linearly with increasing density. However, in the analytical model, the ion throughput does increase as $T_i^{5/2}$ due to the increase in ion velocity and the decrease in ion collisionality with T_i, at least in the regime where the ion-neutral collisions are negligible. Numerical simulation results for throughput vs. simplified analytical modeling for a PMFX type device are illustrated in Fig. 12. At low ion temperatures ($T_i < 3\,eV$), the throughput is near the theoretical maximum (blue line). The simulated throughput continues to increase up to $T_i \geq 10\,eV$, although not as fast as expected from the collisional model.

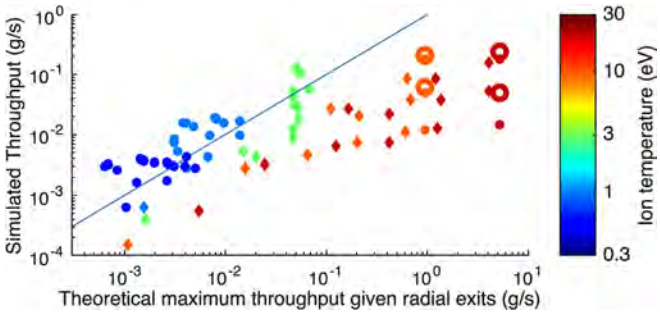

FIG. 12. Simulated throughput vs. analytical model for throughput in a specific mass filter design. At low ion temperatures ($T_i < 3\,eV$), the throughput is near the theoretical maximum (blue line). The simulated throughput continues to increase up to $T_i \geq 10\,eV$, although not as fast as expected from the simplified collisional model. Reprinted with permission from Phys. Plasmas **24**, 043503 (2017). Copyright 2017 AIP Publishing LLC.

An important general conclusion from this analysis is that higher throughput can be obtained by increasing the ion temperature. However, if the resulting $T_i \gg T_e$ (as seems likely), then there may be a significant issue in maintaining this temperature difference in the presence of collisional energy exchange.

IV. GENERIC TECHNOLOGY ISSUES

Since the purpose of this tutorial is to help define a practical plasma mass separation device, some of the generic technological issues are described briefly in this section. Further details, especially concerning the nuclear waste aspects of plasma separation, are discussed in Ref. 162.

A. Plasma source

The material input and ionization sections constitute the plasma source of a mass separation device, as illustrated in Fig. 1. These sections need to convert a solid (or liquid) input stream into a singly ionized plasma, which can then be coupled directly to the main separation chamber. There are many existing techniques to accomplish this for mass analyzers[11,12] and ion beam sources,[125] but only at a relatively low throughput. The challenge for a high throughput plasma mass separation device is to do this with high energy efficiency without the creation of large particles (Sec. III E) or plasma fluctuations (Sec. III H).

A good solution for moderate throughput is the sputtering target developed for ICRH-driven ion separation devices such as shown in Fig. 2.[4,20] Ion sputtering is already used for

industrial applications, such as RF-driven plasma devices for semiconductor etching[77,126] and magnetron sputtering devices for creating thin films.[127,128] Normally, the ionization fractions in sputtering are only ~1%, and the neutral atoms are ejected with a moderate energy, e.g., ~20 eV. Thus, the mean-free-path of these neutrals would have to carry them to a separate ionization section near the target, such as driven by ECRH in Fig. 2. Neutral sputtering rates can be up to ~1 atom/ion, and so, this source process is limited by the ion current to the target. If the plasma density at the target surface is $n = 10^{13}\,cm^{-3}$ and the incident ion speed is $v_i \sim 3 \times 10^6$ cm/s (e.g., Ar^+ at 400 eV), the incident ion flux can be $\sim 3 \times 10^{19}$ ions/cm^2-sec, corresponding to a sputtering rate of ~3 mg/cm^2-s for target atoms of M ~ 60 (but this would add 400 eV to the energy cost/atom of the separation).

An alternative plasma source is a pulsed vacuum arc, which is used for ion implantation and accelerator ion sources[129–131] and in experiments in plasma centrifuges (Sec. II C). These arcs are usually formed in ≤1 ms between two metallic electrodes at a pressure $\leq 10^{-6}$ bar, and ions are created at tiny cathode spots along with metal plasma, neutral gas, and solid particles. Ion energies can be as low as ~20–50 eV, and mean ion charge states are +1 to +3, depending on the species.[91,129] However, most of the ejected material from the arc is in the form of uncharged macroparticles,[132] and the vacuum arc is usually unstable. Some of these difficulties were overcome using a crucible heated by a diffuse arc,[49] which produced for example a gadolinium ion flux of ≤3 mg/s with an average ion charge of near +1. Light and heavy metal components (e.g., Fe and W) in a vacuum arc system with a curved magnetic field were successfully separated using a centrifugal force mechanism,[38] and this could be useful for spent nuclear fuel, especially with macroparticle filtration[105] or with a hot refractory anode vacuum arc.[106–108,133]

There are several other options for creating neutral atoms or molecules from the source target. High energy electron beams can evaporate any material[134] and are commercially used for vacuum welding at up to ~150 kW.[135] High powered infrared lasers up to ~20 kW are used for cutting and machining,[136] but at relatively high cost compared to electron beams. The input stream could also be ground into powder and vaporized, as described for spent nuclear fuel processing in Ref. 6. Calculations of dust evaporation rates[137] suggest that a dust feed stream needs to be of sub-micron size to evaporate within ≤10 ms but that the energy required is only ~5–15 eV/atom. A preliminary test of an aluminum oxide dust dropper in the PMFX experiment was inconclusive,[43] perhaps because the dust became charged and was deflected by E or B fields, as in dusty plasmas.[138]

Most of these atom sources will require supplementary ionization of the neutral atoms. The simplest method is electron cyclotron heating, which can be done inexpensively at 2.45 GHz (microwave oven frequency) at B = 875 G.[139] Other common plasma sources use inductive or capacitive RF or helicon discharges, typically at 13.56 MHz.[77] The efficient coupling of this RF power to large-volume sources is nontrivial but extensively studied.[36,37,68,116,122] An alternative ionization method could be based on large-area heated and biased cathodes to form low energy electron beams (~50–100 V), which can thermalize over short distances.[116,140,141] There are also several other methods of ionization used in conventional mass spectrometers which might possibly be adapted for high throughput, such as electrospray ionization, soft laser desorption, chemical ionization, photoionization, field ionization, thermal ionization, spark sources, and glow discharge sources.[11,12]

B. Plasma heating

Most plasma mass separation mechanisms will require dedicated heating systems to control the ion and electron temperature downstream from the plasma source. In particular, the desire for singly ionized species (Sec. III A) implies that the electron temperature should be roughly $T_e \sim 1$–2 eV, while the desire for high ion throughput suggests that the ion temperature should be $T_i \geq 10$ eV (see Sec. III K). This combination will not occur with electron heating alone, and so, a dedicated ion heating system may be required.

Some RF electron heating methods such as ECRH were mentioned in the discussion of ionization at the end of Sec. IV A. The total RF heating power needed to maintain $T_e \sim 2$ eV depends on the ionization energy (typically 5–15 eV/atom or molecule), atomic radiation loss (Sec. III I), plasma energy loss (Sec. III J), and the efficiency of RF coupling (roughly 0.5). If this energy was a total of ~1 keV/atom, then for a throughput of ~1 g/s (or $\sim 10^{22}$ atoms/s for M = 60), this would require ~1 MW of RF heating. Small linear helicon plasma experiments can operate with only ~1–2 kW of RF power and obtain $T_e \sim 5$ eV, but at $T_i < 1$ eV.[43,69,116,122] A large ~3–4 MW, 6 MHz helicon heating system was developed for the Archimedes device,[36] and a 330 kW RF heating system is being used for a plasma material test facility Proto-MPEX.[142] The main issue in electron heating will be to control the electron temperature profile in order to maintain a dominant charge state of Z = 1 in most of the volume.

Ion energy losses will be due to ion loss to the wall, charge exchange loss, and ion-electron collisional coupling (assuming $T_i > T_e$). The most commonly cited ion heating method for plasma mass separation is ICRH, which is reviewed extensively in the Russian literature.[4,7,31] Ion temperatures of $T_i \sim 10$ eV as measured by the ArII line have also been obtained with ICRH (plus helicon waves) in Proto-Proto-MPEX,[143] and up to $T_i \sim 100$ eV was obtained using single-pass ICRH in deuterium in the VASMIR plasma thruster experiment at ~20 kW.[144] ICRH systems are used in magnetic fusion at power levels of ≥20 MW in D-T plasmas, but mainly for ions with $T_i \gg 1$ keV.[145]

A significant issue in any RF heating system is the practical difficulty of coupling RF power to the plasma in the presence of material deposition on the interior vessel walls. If the RF antennas were just outside an insulating glass or ceramic vessel section, then conducting coatings could shield the RF waves from the plasma. If the antennas were inside the vessel, even thin coatings could lead to shielding or arcing. Thus, techniques to avoid or remove such coatings would have to be developed. High power RF antennas would

probably also need to be actively cooled for steady-state operation, which can be done using water cooled copper tubes.

There are some non-RF plasma heating methods which might also be useful. Resistive Ohmic heating of electrons can be driven by biased electrodes, as in pulsed arc centrifuges (Sec. II C) or heated cathodes.[116,141] In general, resistive heating is a simpler technology than RF heating, but less powerful and less controllable. Electrodes inside the vacuum vessel would probably suffer from erosion and/or coatings, which can limit their lifetime, and they may also need to be actively cooled, which presents safety issues. Another method for ion heating such as proposed for the Archimedes and MCMF devices is through plasma $E \times B$ rotation, which can produce ion speeds comparable to $T_i = 10\,eV$ with modest electric fields of $\sim 3\,V/cm$ at $B = 1\,kG$. These ions would have a velocity perpendicular to B, but this could be directly useful for gyro-orbit separation.[3] Ion acceleration by electric fields has also been observed in several types of DC plasma thrusters for space applications, for example, in an expanding plasma nozzle in VASIMR[146] or Hall thrusters.[147]

C. Material handling

All materials for plasma mass separation will have to be mechanically transferred into and out of the vacuum system, which probably cannot be done during plasma operation. For a moderate throughput of 1 g/s, this will involve handling $\sim 100\,kg/day$. Some of the proposed materials such as spent nuclear fuel and nuclear waste are radioactive and/or toxic; if so, this handling will have to be monitored and controlled very carefully.

Plasma mass separation devices will require significant vacuum pumping, especially if the source material contains oxides or other molecules which can form gaseous products. The vacuum system interior would need to be cleaned frequently to remove coatings on all exposed surfaces, especially on high voltage electrodes or RF antennae. Conventional high vacuum pumps (e.g., rotary mechanical or turbo pumps) are not designed to handle dust, which would have to be carefully filtered out to avoid pump damage. Most plasma mass separators would use strong magnetic fields, and so, iron and other magnetic species may be affected by these fields, at least in solids below the Curie temperature. It is interesting to note that the original calutron uranium separation tanks were cleaned by hand using scrapers and wire brushes,[13] which would probably not be acceptable today.

The most aggressive application of this technology for nuclear waste separation will probably need to be done with remotely controlled devices. The average radiation level of Hanford tank waste is on the order of $\sim 1\,Ci/kg$, mainly from ^{137}Cs and ^{90}Sr, although some of this radioactive waste might be removed by chemical processes before plasma separation. However, even a small amount of radioactive material would contaminate the vacuum chamber, interlocks, and pumps with surface coatings or dust. Further discussion of the nuclear waste issues can be found in Refs. 3 and 162.

V. DIRECTIONS FOR FURTHER RESEARCH

This section outlines possible research directions for developing a useful plasma mass separation device. The general goal is to create a practical device which can make a coarse separation of high mass from low mass atoms or molecules with a range of separation factors and throughputs as shown in Table I. However, here we focus on optimizing the physics and designing experiments, rather than on any specific application.

A. Criteria for evaluating separation mechanisms

Given the wide range of possible separation mechanisms (Sec. II) and the long history of previous experiments (Table II), it is helpful to have criteria to evaluate the proposed research directions. Some useful criteria discussed in this section are history, simplicity, robustness, throughput, efficiency, and cost.

The plasma separation mechanism with the most extensive history is gyro-orbit separation, which was the basis of the calutron and several ion cyclotron resonance separation devices (Sec. II A). This method has produced useful isotope separation, although at relatively low throughput and high cost. The plasma centrifuge was tried several times (Sec. III C) but has many difficulties, as reviewed in Ref. 31. At the other extreme, there have been few successful tests of plasma separation using drift orbits (Sec. II B) or plasma rotation with electrodes (Sec. II D). For example, the Archimedes experiment was based on controlled rotation,[32–36] but no conclusive evidence of separation was reported in the literature.

Simpler physical mechanisms are preferable because they are more likely to work as expected. The gyro-orbit mechanism (Sec. II A) is based on the simplest ion property, and the ion drift orbit mechanism (Sec. II B) is nearly as simple. Another simple mechanism is based on the ionization threshold (Sec. II J), which is well-known atomic physics. At the other extreme, the mechanisms which involve electric fields and/or plasma rotation (e.g., Secs. II C–II E and II I) are complex because the physics of plasma conductivity is not well understood, despite the fact that $E \times B$ rotation is observed in nearly all plasma devices.

Robustness concerns the reliability of the technology associated with each concept. In general, the most robust concepts are likely to be those with the simplest geometry, the lowest magnetic fields, the fewest high voltage components (which are prone to failure), and the fewest in-vacuum systems (which are difficult to maintain). However, many of these features will probably be necessary for a practical system. The more robust concepts include the ion drift orbit separation in a curved magnetic field (Sec. II B) and transit-time separation (Sec. II K), which require low magnetic fields and minimal in-vessel electrodes. The less robust concepts involve pulsed high-voltage electrodes, such as the plasma arc centrifuge (Sec. II C), or high power RF, especially when the antennas are inside the vacuum vessel (Sec. II A).

High throughput is always desirable, but separation efficiency should be optimized for the specific application. Quantitative theoretical metrics for comparing plasma mass filters have been discussed previously,[64] but there is limited

information on the actual performance of relevant systems. Large area devices are preferable for high throughput, which suggests a preference for low magnetic fields. Pulsed systems will generally have lower throughput than steady-state mechanisms. Separation based on ionization potential may have a high throughput but would be limited to separating a small number of species.

The ultimate criterion for practical application is cost. Some attempt has been made to evaluate the energy cost for various plasma separation systems,[3] with an approximate upper bound of 2 GJ/kg or 2 keV/atom for 100 amu, which for an electricity cost of $0.12/kW-hr is about $65/kg. Thus, it is clear that plasma separation would be practical only for fairly high-value source materials. It is important to note that before focusing on an applied plasma separation program, a careful analysis of conventional physical and chemical separation options should be done first since these techniques may be easier and less costly than plasma separation, although plasma separation may have a smaller environmental footprint.

B. Small-scale experiments

After the criteria in Sec. V A are considered with respect to a specific application, it is necessary to test the best concept(s) with experiments. Of course, this step has already been taken in many cases, as shown in Table II, but this did not usually lead to a practical device. An important general question is: what is the smallest experiment which can provide useful test data for evaluating the prospects for meeting the separation and throughput goals at larger scales?

Two good criteria for designing a small-scale plasma separation experiment are that the mechanism of choice should be dominant and that quantitative measurements should be performed to compare the separation results with theoretical models. As counterexamples, the PMFX experiment[43] was useful to test the response of the plasma to electrode biasing, but the gyro-orbit separation mechanisms of interest were not dominant due to the high collisionality; the Archimedes experiment[36] may have had parameters suitable for demonstrating separation, but separation results were not published (perhaps because of proprietary interest). Probably, the most successful technology for plasma separation has been the ICRH gyro-orbit devices, which were started at a small-scale[19] and evolved into large devices which had practical applications for isotope separation,[4,90] but the application of this method to SNF processing could be extremely difficult.

An approximate set of parameters for initial small-scale experiments is given in Table III. Initial separation tests can be done with inert (wall recycling) gases or molecular (non-recycling) gases such as sulfur dioxide or even (toxic) gases such as tungsten hexafluoride. Metals or metal oxides can be injected using ion sputtering, laser-blow-off, electric sparks, or powder droppers (see Sec. IV A). A valuable small-scale separation experiment could be done using ICRH with light elements. It is important that good diagnostics be available to measure the separation efficiency and throughput, as well as the plasma physics parameters (see Sec. V D). Existing linear experiments have studied some of the plasma physics issues such as electric fields and fluctuations [e.g., Refs. 67–69, 116, and 122], but the physics of such devices is still under investigation. Despite the good experiments in Table II and others, the physics of ion mass separation in plasmas is not yet well enough understood to make an efficient high throughput device. Thus, there is a considerable scope for interesting small-scale experiments in this area.

After a small-scale experiment demonstrates a promising technique for plasma mass separation at a low throughput (~1–10 mg/s), a medium-scale experiment could be designed with the help of theoretical simulations (see Sec. V C). This would require a much larger plasma volume and heating power but is necessary in order to evaluate the practical issues of energy balance, coating of internal components, and reliable throughput.

C. Theory and simulation

Each of the plasma separation mechanisms of Sec. II is based on a simple theoretical idea but few if any of them have been analyzed systematically with respect to all of the physics issues discussed in Sec. III. Obviously, a research program would benefit from detailed theoretical simulations of how these ideas would play out in a realistic system. Codes would be needed in at least four distinct areas: atomic physics, particle transport, plasma dynamics, and plasma technology.

There are several crucial issues involving atomic physics which need to be clarified for any plasma separation device; for example, the ion charge state balance, atomic radiation level, molecular ion state, and charge exchange/recombination rates. Given the unusual atomic composition of most applications (Table II), it is possible that many of these rates will have to be derived or approximated especially for this code. The basic inputs would be the species mix exiting from the plasma source and the assumed plasma electron density and temperature profiles in the separation volume. The outputs would be the ion charge state distribution for each species (including neutrals), the molecular composition (including positive and negative ions), and the local radiated power (needed for the system energy balance). These outputs would be used to define the possible operating points, e.g., where the important species are singly charged and the radiated power is manageable. The assumptions of Maxwellian electron and ion distribution functions and an equilibrium ion charge state distribution should be questioned, especially for any marginally collisionless device. Thus, a quantitative model for the atomic physics in a plasma separation device will be extremely complicated and may not provide accurate predictive capabilities.

The central physics issue in any plasma separation device is the transport of ions from the source to the heavy and the light-atom output streams (Fig. 1). Thus, the motion of particle species should be simulated in a realistic geometry, including the ionized atoms and molecules, the neutral atoms and molecules, and any larger particles such as dust in the system. The particle transport code which does this should have the physics of the separation mechanism (e.g., the ion orbits and drifts in a magnetic field), all relevant

collision processes (e.g., ion-neutral collisions and charge exchange), and the electric and magnetic fields which influence the particle motion (preferably calculated self-consistently with the transport). The basic inputs to this code would be the assumed particle species, the assumed plasma parameters, and the relevant electric and magnetic fields (excluding fluctuations). The output would be an idealized first-approximation to the particle throughput and separation efficiency, including an inventory of where each type of atom will ultimately strike the wall inside the vacuum chamber. To be realistic, this code should also be coupled to a particle source model and a particle exhaust model. The transport of neutral particles will be important, even though they will not be directly affected by the separation mechanisms.

Perhaps the most difficult issue to treat in a code is the plasma dynamics, i.e., the plasma motion and fluctuations, as discussed in Secs. III G and III H. For example, if the plasma is unstable on the timescale of the ion separation process, then the collisional model for particle transport can be overwhelmed by unstable flows or turbulent mixing. The basic inputs to a plasma dynamics code would be the assumed plasma density and temperature profiles and the externally applied electric and magnetic fields. The outputs of the code would be the average plasma velocity in 3D, the frequency and wavenumber spectra of the plasma fluctuations, and their approximate transport effects. Existing plasma dynamics codes use fluid MHD, kinetic theory, or particle-pushing, but these usually include non-linear effects and so are computationally expensive and difficult. It is unrealistic to expect that the transport effects can be simulated accurately since this is still not possible for linear plasma experiments or magnetic fusion experiments. However, it may be possible to identify the most stable operating regimes in a specific separation scenario, in order to minimize the fluctuation-induced mixing effects.

A separate code for plasma technology issues will be needed to optimize the plasma source, plasma heating, and material handling, as discussed in Sec. IV. The plasma source code could probably be based on existing devices, e.g., for ion sputtering and ionization. The plasma heating code would be specific to the technologies chosen, for example, based on the fairly well understood ECRH and ICRH interactions. The exhaust processes will depend on the plasma-surface interactions of the ions and recycling and pumping of neutrals. Although these technological issues seem relatively simple compared to the physics issues, they are essential for the successful operation of practical devices.

New theoretical ideas can also be developed to improve plasma mass separation. For example, the Archimedes experiment supported the radial electric field through end electrodes, which define a potential along the axial field lines. However, these electrodes are technologically problematic as they come into contact with the plasma. Moreover, the plasma may short out the voltage near the electrode. An alternative concept to produce a radial potential and rotation is to induce differential transport of ions volumetrically through waves[148] or through passive antenna structures.[149] These ideas draw upon ideas in magnetic fusion for recovering particle energy through wave-induced transport.[150] The transport of ions then leaves behind a negative radial potential. Producing plasma rotation in a technologically robust and economical manner remains an open area for further research.

D. Experimental diagnostics

The plasma diagnostics for a separation experiment can be similar to those on existing linear devices;[67–69,76,116,122] for example, Langmuir probes for density and temperature measurements, Mach probes for rotation and flow measurements, visible spectroscopy for ion velocity and temperature, gridded energy analyzers for ion distribution functions, and a fast camera to see fluctuations. Passive broad-wavelength survey spectrometers can provide qualitative information on the ionization states and approximate location of all the species in the plasma, but quantitative measurements are difficult due to line-integration and the need for electron temperature information to interpret them. Commercial residual gas analyzers would be useful to measure the neutral gas composition in real-time, including points inside the vacuum chamber which could be sampled with movable tubes. But conventional mass spectrometers would have difficulty in measuring the location or concentration of species which are solid at room temperature, which is the main interest in plasma mass separation.

At low throughputs of $\sim$1 mg/s, these solids will form micron-thick films on the inner surfaces of the vacuum vessel. Many diagnostics for thin surface films in vacuum systems have been developed for industrial and fusion applications, and these can be adapted for a plasma separation device. Some other techniques could be used in real time during plasma operation, such as laser ellipsometry[151] or quartz microbalances[152] for measuring the film thickness. Other surface diagnostics could be used *in situ* between plasma pulses (due to background light), such as laser-induced breakdown spectroscopy (LIBS),[153] x-ray fluorescence,[154] or Raman spectroscopy[155] for the surface chemical composition. Ideally, these diagnostics should be able to scan over a wide area inside the vacuum vessel to look for unexpected depositions.

At higher throughputs, the deposition will be macroscopic and could be measured using sample coupons removed from the system with vacuum interlocks and analyzed *ex situ* by standard analytical techniques such as SIMS or x-ray measurements.[22,23,38,39] On the other hand, these thicker films might also coat windows and probes and so could make some of the other diagnostics more difficult; for example, it is difficult to measure the electron temperature with coated Langmuir probes. Some diagnostics of the micron-sized dust in the chamber could also be useful, using laser scattering or other techniques developed for dusty plasmas.[156]

E. Directions for future research

There are many interesting directions for future research toward an optimized high throughout plasma mass separation device. Perhaps, the most fundamental open question concerns the basic physical mechanisms: are there more efficient

separation mechanisms than those discussed in Sec. II? For example, the selective laser excitation of uranium isotopes can improve separation efficiency as in the AVLIS process,[157] and light ions can be separated from heavy ions in a rapidly time-varying magnetic field.[158] Alternatively, separation methods which can create or exploit density differences of dust or droplets in plasmas might be more efficient than atomic or molecular separation since they operate on many atoms at a time. Mechanisms which allow simultaneous separation *of multiple* mass components should be investigated, which could increase the economic value of the output stream. Work in this direction is presently being done with the POMS concept in Irkutsk,[42] the stable isotope production programs at Kurchatov[31] and ORNL,[16] and efforts to separate the elements in spent nuclear fuel.[6,31]

Research is also needed on many of the generic physics issues discussed in Sec. III. More detailed assessments should be made on the charge state distribution, radiation, and charge exchange for species of interest, which can best be done with a dedicated low temperature atomic physics code. Better physical understanding of the electric field penetration and rotation in magnetized plasmas is obviously of interest for many separation techniques and is already a topic of experiments at the basic physics level.[67–69,116,122] Small experiments can be developed to test specific new ideas or to improve existing techniques; for example, a valuable small-scale separation experiment could be done using ICRH with light elements. Medium-scale experiments could be designed with the aid of computational simulation and built to be adaptable for testing several different separation mechanisms using a consistent set of diagnostics. International collaborations on plasma mass separation should be pursued, including for example the substantial expertise in this topic in Russia and France.

Another interesting direction in plasma mass separation is magnetized collisional transport effects in fully ionized plasma, which exploit ion-ion scattering to separate or concentrate ionic species. In fact, the natural collection of impurities in the hot center of magnetic fusion devices such as tokamaks is highly concerning since these impurities may poison the fuel purity and eventually quench the reaction. The impurities tend to collect because the hot center of the tokamak is also the place where the density peaks, and collisions between magnetized ions tend to drive the high-Z_i impurities to have scale lengths Z_i times shorter than the hydrogen majority, where Z_i is the impurity charge state.[159] On the other hand, in magnetized non-neutral plasma, the fast rotation tends to stratify ions according to m_i/Z_i.[160] Rotation effects can also operate in neutral plasma, for example, to separate ash alpha particles in a p-B^{11} fusion reaction, even though the alpha particle, compared to p and B^{11}, has both intermediate mass and intermediate charge.[161] These effects do suggest a direction for interesting separation opportunities. However, because of the high temperature needed to achieve full ionization, and because of radiation losses, this is a direction for the purification of plasma mixtures already brought to high-temperature for other reasons.

F. Summary

In summary, there are many possible mechanisms for plasma mass separation as discussed in Sec. II, and also many interesting physics and technical issues which need to be resolved before a practical separation device can be achieved, as discussed in Secs. III and IV. Although each of these mechanisms is theoretically capable of separating ions of high mass from ions of low mass, the results achieved so far have been at a relatively low throughput at a relatively high cost. Thus, there are many good opportunities for developing new ideas, codes, and experiments to make useful high throughput devices, as discussed in Secs. V A–V E.

ACKNOWLEDGMENTS

We thank the following people who have worked with us on this topic: A. Carpe, D. Cylinder, D. DiCicco, E. Evans, M. Galante, C. Gentile, A. Khodak, F. Levinton, M. Mlodik, I. Ochs, and J. M. Rax. We also thank S. Prager, P. Efthimion, and J. Hosea for supporting this project and K. M. Young for advice on publication. This work was funded by USDOE Contract No. DE-AC02-09CH11466.

[1]W. E. Parkins, Phys. Today **58**(5), 45 (2005).
[2]K. K. Sirkar, *Separation of Molecules, Macromolecules, and Particles* (Cambridge University Press, 2014).
[3]R. Gueroult, J.-M. Rax, S. J. Zweben, and N. J. Fisch, Plasma Phys. Controlled Fusion **60**, 014018 (2018).
[4]D. A. Dolgolenko and Y. A. Muromkin, Phys.-Usp. **52**, 345 (2009).
[5]R. Gueroult, D. T. Hobbs, and N. J. Fisch, J. Hazardous Mater. **297**, 153 (2015).
[6]V. B. Yuferov, S. V. Katrechko, V. O. Ilichova, S. V. Shariy, A. S. Svichkar, M. O. Shvets, E. V. Mufel, and A. G. Bobrov, Probl. At. Sci. Technol. **113**(1), 118–126 (2018).
[7]A. V. Timofeev, Phys.-Usp. **57**, 990 (2014).
[8]R. Gueroult and N. J. Fisch, Plasma Sources Sci. Technol. **23**, 035002 (2014).
[9]R. Gueroult, J. M. Rax, and N. J. Fisch, J. Cleaner Prod. **182**, 1060 (2018).
[10]J. Heberlein and A. B. Murphy, J. Phys. D: Appl. Phys. **41**, 053001 (2008).
[11]J. H. Gross, *Mass Spectroscopy, a Textbook* (Springer, 2011).
[12]E. de Hoffmann and V. Stroobant, *Mass Spectroscopy, Principles and Applications*, 3rd ed. (Wiley, 2007).
[13]A. L. Yergey and A. K. Yergey, J. Am. Soc. Mass. Spectrom. **8**, 943 (1997).
[14]L. P. Smith, W. E. Parkins, and A. T. Forrester, Phys. Rev. **72**, 989 (1947).
[15]P. Maier-Komor, Nucl. Instrum. Methods Phys. Res. A **613**, 465 (2010).
[16]B. J. Egle, K. J. Hart, and W. S. Aaron, J. Radioanal. Nucl. Chem. **299**, 995 (2014).
[17]T. R. Mazur, B. Klappauf, and M. G. Raizen, Nat. Phys. **10**, 601 (2014).
[18]B. Bonnevier, Plasma Phys. **13**, 763 (1971).
[19]J. M. Dawson, H. C. Kim, D. Arnush, B. D. Fried, R. W. Gould, L. O. Heflinger, C. F. Kennel, T. E. Romesser, R. L. Stenzel, A. Y. Wong, and R. F. Wuerker, Phys. Rev. Lett. **37**, 1547 (1976).
[20]A. Compant La Fontaine and V. G. Pashkovsky, Phys. Plasmas **2**, 4641 (1995).
[21]M. Krishnan, M. Geva, and J. L. Hirshfield, Phys. Rev. Lett. **46**, 36 (1981).
[22]M. Geva, M. Krishnan, and J. L. Hirshfield, J. App. Phys. **56**, 1398 (1984).
[23]R. R. Prasad and M. Krishnan, Nucl. Instrum. Methods Phys. Res. B **26**, 65 (1987).
[24]P. J. Evans, F. J. Paoloni, J. T. Noorman, and J. V. Whichello, J. Appl. Phys. **66**, 115 (1989).
[25]M. J. Hole and S. W. Simpson, Phys. Plasmas **4**, 3493 (1997).
[26]M. J. Hole and S. W. Simpson, IEEE Trans. Plasma Sci. **27**, 620 (1999).

[27]E. del Bosco, R. S. Dallaqua, G. O. Ludwig, and J. A. Bittencourt, Appl. Phys. Lett. **50**, 1716 (1987).
[28]E. del Bosco, S. W. Simpson, R. S. Dallaqua, and A. Montes, J. Phys. D: App. Phys. **24**, 2008 (1991).
[29]R. S. Dallaqua, E. del Bosco, R. P. da Silva, and S. W. Simpson, IEEE Trans. Plasma Sci. **26**, 1044 (1998).
[30]M. J. Hole, R. S. Dallaqua, S. W. Simpson, and E. del Bosco, Phys. Rev. E **65**, 046409 (2002).
[31]D. A. Dolgolenko and Y. A. Muromkin, Phys.-Usp. **60**, 994 (2017).
[32]T. Ohkawa and R. L. Miller, Phys. Plasmas **9**, 5116 (2002).
[33]R. Freeman, S. Agnew, F. Anderegg, B. Cluggish, J. Gilleland, R. Isler, A. Litvak, R. Miller, R. O'Neill, T. Ohkawa, S. Pronko, S. Putvinski, L. Sevier, A. Sibley, K. Umstadter, T. Wade, and D. Winslow, AIP Conf. Proc. **694**, 403 (2003).
[34]C. E. Ahlfeld, J. D. Wagoner, D. L. Sevier, and R. L. Freeman, in *Proceedings of 21st IEEE/NPSS Symposium on Fusion Engineering, SOFE 05* (2006), p. 81.
[35]A. Litvak, S. Agnew, F. Anderegg, B. Cluggish, R. Freeman, J. Gilleland, R. Isler, W. Lee, R. Miller, T. Ohkawa, S. Putvinski, L. Sevier, K. Umstadter, and D. Winslow, in *30th EPS Conference on Controlled Fusion and Plasma Physics, St. Petersburg*, 7–11 July 2003, Vol. 27A, paper No. O-1.6A.
[36]B. P. Cluggish, F. A. Anderegg, R. L. Freeman, J. Gilleland, T. J. Hilsabeck, R. C. Isler, W. D. Lee, A. A. Litvak, R. L. Miller, T. Ohkawa, S. Putvinski, K. R. Umstadter, and D. L. Winslow, Phys. Plasmas **12**, 057101 (2005).
[37]S. Shinohara and S. Horii, Jpn. J. Appl. Phys., Part 1 **46**, 4276 (2007).
[38]V. L. Paperny, V. I. Krasov, N. V. Lebedev, N. V. Astrakchantsev, and A. A. Chernikch, Plasma Sources Sci. Tech. **24**, 015009 (2015).
[39]V. L. Paperny, Y. V. Korobkin, V. I. Krasov, and N. V. Lebedev, Contrib. Plasma Phys. **54**, 635 (2014).
[40]V. M. Bardakov, G. N. Kichigin, N. A. Strokin, and E. O. Tsaregorodtsev, Tech. Phys. **55**, 1504 (2010).
[41]V. M. Bardakov, S. D. Ivanov, and N. A. Strokin, Phys. Plasmas **21**, 033505 (2014).
[42]V. M. Bardakov, S. D. Ivanov, A. V. Kazantsev, and N. A. Strokin, Plasma Sci. Technol. **17**, 862 (2015).
[43]R. Gueroult, E. S. Evans, S. J. Zweben, N. J. Fisch, and F. Levinton, Plasma Sources Sci. Tech. **25**, 035024 (2016).
[44]I. Ochs, R. Gueroult, N. J. Fisch, and S. J. Zweben, Phys. Plasmas **24**, 043503 (2017).
[45]V. P. Smirnov, A. A. Samokhin, N. A. Vorona, and A. V. Gavrikov, Plasma Phys. Rep. **39**, 456 (2013).
[46]A. A. Samokhin, V. P. Smirnov, A. V. Gavrikov, and N. A. Vorona, Tech. Phys. **61**, 283 (2016).
[47]N. A. Vorona, A. V. Gavrikov, A. A. Samokhina, V. P. Smirnov, and Y. S. Khomyakov, Phys. At. Nucl. **78**, 1624 (2015).
[48]A. V. Gavrikov, N. A. Vorona, G. D. Liziakin, R. A. Usmanov, O. O. Samoylov, V. P. Smirnov, and R. A. Timirhanov, J. Phys.: Conf. Ser. **774**, 012197 (2016)
[49]R. K. Amirov, N. A. Vorona, A. V. Gavrikov, G. D. Lizyakin, V. P. Polishchuk, I. S. Samoilov, V. P. Smirnov, R. A. Usmanov, and I. M. Yartsev, Plasma Phys. Rep. **41**, 808 (2015).
[50]R. K. Amirov, N. A. Vorona, A. V. Gavrikov, G. D. Liziakin, V. P. Polistchook, I. S. Samoylov, V. P. Smirnov, R. A. Usmanov, and I. M. Yartsev, Phys. At. Nucl. **78**, 1631 (2015).
[51]H. P. Eubank and T. D. Wilkerson, Phys. Fluids **6**, 914 (1963).
[52]V. S. Voitsenya, A. G. Gorbanyuk, I. N. Onishchenko, and B. G. Safronov, Sov. Phys.-Tech. Phys. **9**, 221 (1964).
[53]S. Ejima, T. C. Marshall, and S. P. Schlessinger, Phys. Fluids **17**, 163 (1974).
[54]A. Komori, N. Sato, H. Sugai, and Y. Hatta, Plasma Phys. **19**, 283 (1977).
[55]R. Gueroult and N. J. Fisch, Phys. Plasmas **19**, 112105 (2012).
[56]K. W. Gentle and H. Huang, Plasma Sci. Technol. **10**, 284 (2008).
[57]T. Ikehata, K. Oohashi, N. Y. Sato, T. Tanabe, and H. Mase, Nucl. Instrum. Methods Phys. Res. B **70**, 26 (1992).
[58]R. Dux, A. G. Peeters, A. Gude, A. Kallenbach, R. Neu, and ASDEX Upgrade Team, Nucl. Fusion **39**, 1509 (1999).
[59]H. Chen, N. C. Hawkes, L. C. Ingesson, M. von Hellermann, K. D. Zastrow, M. G. Haines, M. Romanelli, and N. J. Peacock, Phys. Plasmas **7**, 4567 (2000).
[60]W. Guss, https://digital.library.unt.edu/ark:/67531/metadc678026/ for "The plasma centrifuge: A compact, low cost, stable isotope separator," 1996.
[61]J.-M. Rax and R. Gueroult, J. Plasma Phys. **82**, 595820504 (2016).
[62]R. Gueroult, J. M. Rax, and N. J. Fisch, Phys. Plasmas **21**, 020701 (2014).
[63]C. Teodorescu, R. Clary, R. F. Ellis, A. B. Hassam, C. A. Romero-Talamas, and W. C. Young, Phys. Plasma **17**, 052503 (2010).
[64]A. J. Fetterman and N. J. Fisch, Phys. Plasmas **18**, 094503 (2011).
[65]R. Gueroult and N. J. Fisch, Phys. Plasmas **19**, 122503 (2012).
[66]A. J. Fetterman and N. J. Fisch, Phys. Plasmas **18**, 103503 (2011).
[67]C. Holland, J. H. Yu, A. James, D. Nishijima, M. Shimada, N. Taheri, and G. R. Tynan, Phys. Rev. Lett. **96**, 195002 (2006).
[68]E. Scime, R. Hardin, C. Biloiu, A. M. Keesee, and X. Sun, Phys. Plasmas **14**, 043505 (2007).
[69]S. C. Thakur, J. J. Gosselin, J. McKee, E. E. Scime, S. H. Sears, and G. R. Tynan, Phys. Plasmas **23**, 082112 (2016).
[70]I. E. Ochs, J. M. Rax, R. Gueroult, and N. J. Fisch, Phys. Plasmas **24**, 083503 (2017).
[71]S. Hirshman and D. Sigmar, Nucl. Fusion **21**, 1079 (1981).
[72]V. Rozhansky, Phys. Plasmas **20**, 101614 (2013).
[73]A. Fasoli, F. Skiff, T. N. Good, and P. J. Paris, Phys. Rev. Lett. **68**, 2925 (1992).
[74]A. Perry, G. Conway, R. Boswell, and H. Persing, Phys. Plasmas **9**, 3171 (2002).
[75]J. P. Boeuf, B. Chaudhury, and L. Garrigues, Phys. Plasmas **19**, 113509 (2012).
[76]M. U. Siddiqui, D. S. Thompson, J. M. McIlvain, Z. D. Short, and E. E. Scime, Phys. Plasmas **22**, 122103 (2015).
[77]M. A. Lieberman and A. J. Lichtenberg, *Principles of Plasma Discharge for Materials Processing* (John Wiley & Sons, 1994).
[78]X. Wang and N. Hershkowitz, Phys. Plasmas **13**, 053503 (2006).
[79]A. B. Kanu, P. Dwivedi, M. Tam, L. Matz, and H. H. Hill, Jr., J. Mass Spectrosc. **43**, 1 (2008).
[80]H. Borsdorf, T. Mayer, M. Zarejousheghani, and G. A. Eiceman, Appl. Spectrosc. Rev. **46**, 472 (2011).
[81]A. Ezoubtchenko, N. Ohtsuki, H. Akatsuka, and M. Suzuki, Plasma Sources Sci. Technol. **7**, 136 (1998).
[82]B. Bonnevier, Astrophys. Space Sci. **40**, 231 (1976).
[83]G. T. Marklund, Nature **277**, 370 (1979).
[84]See http://www.lenntech.com/periodic-chart-elements/ionization-energy.htm for Ionization energies.
[85]R. E. Steiner, C. L. Lewis, and V. Majidi, J. Anal. At. Spectrom. **14**, 1537 (1999).
[86]A. Gundlach-Graham, E. A. Dennis, S. J. Ray, C. G. Enke, C. J. Barinaga, D. W. Koppenaalc, and G. M. Hieftje, J. Anal. At. Spectrom. **28**, 1385 (2013).
[87]H.-K. Chung, M. H. Chen, W. L. Morgan, Y. Ralchenko, and R. W. Lee, High Energy Density Phys. **1**, 3 (2005).
[88]D. E. Post and R. V. Jensen, At. Data Nucl. Data Tables **20**, 397 (1977).
[89]See http://open.adas.ac.uk/ for Atomic Data and Analysis Structure (ADAS).
[90]F. F. Chen, "Double helix: the Dawson separation process," in *From Fusion to Light Surfing*, edited by T. Katsouleas (Addison-Wesley, New York, 2011), Ch. 14.
[91]A. Anders, Phys. Rev. E **55**, 969 (1997).
[92]I. Joseph, M. E. Rensink, D. P. Stotler, A. M. Dimits, L. L. LoDestro, G. D. Porter, T. D. Rognlien, B. Sjogreen, and M. V. Umansky, J. Nucl. Mat. Energy **12**, 813 (2017).
[93]D. P. Stotler, F. Scotti, R. E. Bell, A. Diallo, B. P. LeBlanc, M. Podestà, A. L. Roquemore, and P. W. Ross, Phys. Plasmas **22**, 082506 (2015).
[94]A. Fridman, *Plasma Chemistry* (Cambridge University Press, 2008).
[95]See http://webbook.nist.gov/chemistry/ie-ser/ for NIST Chemistry Webbook.
[96]K. Watanabe, T. Nakayama, and J. Mottl, J. Quant. Spectrosc. Radiat. Transfer **2**, 369 (1962).
[97]L. Yu-Ran, *Comprehensive Handbook of Chemical Bond Energies* (CRC Press, 2007).
[98]M. J. Kushner, J. Appl. Phys. **63**, 2532 (1988).
[99]R. S. Devoto, Phys. Fluids **16**, 616 (1973).
[100]D. Rapp and W. E. Francis, J. Chem. Phys. **37**, 2631 (1962).
[101]See https://www-amdis.iaea.org/ALADDIN/collision.html for ALADDIN database.
[102]See http://www.sciencedirect.com/science/journal/0092640X?sdc=1 for ADND Tables.
[103]L. C. Pitchford, J. Phys. D: Appl. Phys. **46**, 330301 (2013).

[104]D. A. Hayton and B. Peart, J. Phys. B: At. Mol. Opt. Phys. **28**, L279 (1995).
[105]I. I. Beilis, M. Keidar, R. L. Boxman, and S. Goldsmith, J. Appl. Phys. **85**, 1358 (1999).
[106]I. I. Beilis and R. L. Boxman, Surf. Coat. Technol. **204**(N6-7), 865 (2009).
[107]I. I. Beilis, Y. Koulik, and R. L. Boxman, IEEE Trans. Plasma Sci. **39**(N11, Part 1), 2838 (2001).
[108]I. I. Beilis, Y. Koulik, and R. L. Boxman, Surf. Coat. Technol. **258**, 908 (2014).
[109]S. Jaiswal, P. Bandyopadhyay, and A. Sen, Rev. Sci. Instrum. **86**, 11 (2015).
[110]E. Thomas and M. Watson, Phys. Plasmas **6**, 4111 (1999).
[111]R. L. Merlino, A. Barkan, C. Thompson, and N. D'Angelo, Phys. Plasmas **5**, 1607 (1998).
[112]T. Ditmire, T. Donnelly, A. M. Rubenchik, R. W. Falcone, and M. D. Perry, Phys. Rev. A **53**, 3379 (1996).
[113]A. S. Boldarev, A. Y. Faenov, Y. Fukuda, S. Jinno, T. A. Pikuz, M. Kando, K. Kondo, and R. Kodama, Laser Part. Beams **35**, 397 (2017).
[114]S. Yatom, J. Bak, A. Khrabryi, and Y. Raitses, Carbon **117**, 154 (2017).
[115]See https://www-amdis.iaea.org/databases.php for Atomic Molecular Data Services.
[116]M. Gilmore, A. G. Lynn, T. R. Desjardins, Y. Zhang, C. Watts, S. C. Hsu, S. Betts, R. Kelly, and E. Schamiloglu, J. Plasma Phys. **81**, 345810104 (2015).
[117]M. U. Siddiqui, D. S. Thompson, C. D. Jackson, J. F. Kim, N. Hershkowitz, and E. E. Scime, Phys. Plasmas **23**, 057101 (2016).
[118]R. R. Weynants and G. Van Oost, Plasma Phys. Controlled Fusion **35**, B177 (1993).
[119]P. Vaezi, C. Holland, S. C. Thakur, and G. R. Tynan, Phys. Plasmas **24**, 042306 (2017).
[120]R. M. Churchill, C. S. Chang, S. Ku, and J. Dominski, Plasma Phys. Controlled Fusion **59**, 105014 (2017).
[121]D. Bohm, *The Characteristics of Electrical Discharges in Magnetic Fields*, edited by A. Guthrie and R. K. Wakerling (McGraw-Hill, New York, 1949).
[122]E. E. Scime, P. A. Keiter, M. M. Balkey, J. L. Kline, X. Sun, A. M. Keesee, R. A. Hardin, I. A. Biloiu, S. Houshmandyar, S. C. Thakur, J. Carr, Jr., M. Galante, D. McCarren, and S. Sears, J. Plasma Phys. **81**, 345810103 (2015).
[123]R. Gueroult, J. M. Rax, and N. J. Fisch, Phys. Plasmas **24**, 082102 (2017).
[124]P. C. Stangeby, *The Plasma Boundary of Magnetic Fusion Devices* (Taylor and Francis, 2000).
[125]I. G. Brown, *The Physics and Technology of Ion Sources*, 2nd ed. (Wiley, 2004).
[126]J. Hopwood, Plasma Sources Sci. Technol. **1**, 109 (1992).
[127]P. J. Kelly and R. D. Arnell, Vacuum **56**, 159 (2000).
[128]K. Sarakinos, J. Almai, and S. Konstantinidis, Surf. Coat. Technol. **204**, 1661 (2010).
[129]I. G. Brown, Rev. Sci. Instrum. **65**, 3061 (1994).
[130]P. Siemroth, T. Schulke, and T. Witke, Surf. Coat. Technol. **68/69**, 314 (1994).
[131]A. Anders *et al.*, IEEE Trans. Plasma Sci. **33**, 1532 (2005).
[132]R. L. Boxman and S. Goldsmith, Surf. Coat. Technol. **52**, 39 (1992).
[133]I. I. Beilis, S. Goldsmith, and R. L. Boxman, Surf. Coat. Technol. **133-134**, 91 (2000).
[134]D. M. Goebel and R. M. Watkins, Rev. Sci. Instrum. **71**, 388 (2000).
[135]See https://www.ptreb.com/electron-beam-welders-and-systems for e-beam welders.
[136]See https://www.trumpf.com/en_US/products/machines-systems/laser-cutting-machines/ for laser cutters.
[137]Y. Tanaka, A. Yu. Pigarov, R. D. Smirnov, S. I. Krasheninnikov, N. Ohno, and Y. Uesugi, Phys. Plasmas **14**, 052504 (2007).
[138]A. Melzer and J. Goree, *Fundamentals of Dusty Plasmas, in Low Temperature Plasmas Fundamentals, Technologies and Techniques* (Wiley, 2007).
[139]J. H. Bowles, D. Duncan, D. N. Walker, W. E. Amatucci, and J. A. Antoniades, Rev. Sci. Instrum. **67**, 455 (1996).
[140]S. K. Matoo, V. P. Anitha, L. M. Awasthi, G. Ravi, and LVPD Team, Rev. Sci. Instrum. **72**, 3864 (2001).
[141]W. Gekelman, P. Pribyl, Z. Lucky, M. Drandell, D. Leneman, J. Maggs, S. Vincena, B. Van Compernolle, S. K. P. Tripathi, G. Morales, T. A. Carter, Y. Wang, and T. DeHaas, Rev. Sci. Instrum. **87**, 025105 (2016).
[142]J. Rapp, T. M. Biewer, T. S. Bigelow, J. F. Caneses, J. B. O. Caughman, S. J. Diem, R. H. Goulding, R. C. Isler, A. Lumsdaine, C. J. Beers, T. Bjorholm, C. Bradley, J. M. Canik, D. Donovan, R. C. Duckworth, R. J. Ellis, V. Graves, D. Giuliano, D. L. Green, D. L. Hillis, R. H. Howard, N. Kafle, Y. Katoh, A. Lasa, T. Lessard, E. H. Martin, S. J. Meitner, G.-N. Luo, W. D. McGinnis, L. W. Owen, H. B. Ray, G. C. Shaw, M. Showers, V. Varma, and the MPEX Team, Nucl. Fusion **57**, 116001 (2017).
[143]C. J. Beers, R. H. Goulding, R. C. Isler, E. H. Martin, T. M. Biewer, J. F. Caneses, J. B. O. Caughman, N. Kafle, and J. Rapp, Phys. Plasmas **25**, 013526 (2018).
[144]E. A. Bering, F. R. Chang-Diaz, J. P. Squire, M. Brukardt, T. W. Glover, R. D. Bengtson, V. T. Jacobson, G. E. McCaskill, and L. Cassady, Adv. Space Res. **42**, 192 (2008).
[145]D. F. H. Start, J. Jacquinot, V. Bergeaud, V. P. Bhatnagar, S. W. Conroy, G. A. Cottrell, S. Clement, G. Ericsson, L.-G. Eriksson, A. Fasoli, V. Fuchs, A. Gondhalekar, C. Gormezano, G. Gorini, G. Grosshoeg, K. Guenther, P. J. Harbour, R. F. Heeter, L. D. Horton, A. C. Howman, H. J. Jackel, O. N. Jarvis, J. Kallneb, C. N. Lashmore Davies, K. D. Lawson, C. G. Lowry, M. J. Mantsineni, F. B. Marcus, R. D. Monk, E. Righi, F. G. Rimini, G. J. Sadler, G. Saibene, R. Sartori, B. Schunke, S. E. Sharapov, A. C. C. Sips, M. F. Stamp, M. Tardocchi, and P. van Belle, Nucl. Fusion **39**, 321 (1999).
[146]B. W. Longmier, E. A. Bering III, M. D. Carter, L. D. Cassady, W. J. Chancery, F. R. Chang Dıaz, T. W. Glover, N. Hershkowitz, A. V. Ilin, G. E. McCaskill, C. S. Olsen, and J. P. Squire, Plasma Sources Sci. Technol. **20**, 015007 (2011).
[147]N. J. Fisch, Y. Raitses, and A. Fruchtman, Plasmas Phys. Controlled Fusion **53**, 124038 (2011).
[148]A. J. Fetterman and N. J. Fisch, Phys. Rev. Lett. **101**, 205003 (2008).
[149]A. J. Fetterman and N. J. Fisch, Phys. Plasma **17**, 042112 (2010).
[150]N. J. Fisch and J.-M. Rax, Phys. Rev. Lett. **69**, 612–615 (1992).
[151]I. P. Herman, Annu. Rev. Phys. Chem. **54**, 277 (2003).
[152]C. H. Skinner, H. Kugel, A. L. Roquemore, J. Hogan, W. R. Wampler, and the NSTX Team, J. Nucl. Mater. **337-339**, 129 (2005).
[153]D. W. Hahn and N. Omenetto, Appl. Spectrosc. **66**, 347 (2012); **64**, 335A (2010).
[154]P. J. Potts and P. C. Webb, J. Geochem. Explor. **44**, 251 (1992).
[155]J. R. Ferraro, K. Nakamoto, and C. W. Brown, *Introductory Raman Spectroscopy*, 2nd ed. (Elsevier, 2003).
[156]B. A. Annaratone, W. Jacob, C. Arnas, and G. E. Morfill, IEEE Trans. Plasma Sci. **37**, 270 (2009).
[157]M. W. Grossman and T. A. Shepp, IEEE Trans. Plasma Sci. **19**, 1114 (1991).
[158]A. Weingarten, R. Arad, Y. Maron, and A. Fruchtman, Phys. Rev. Lett. **87**, 115004 (2001).
[159]J. B. Taylor, Phys. Fluids **4**, 1142 (1961).
[160]T. M. O'Neill, Phys. Fluids **24**, 1447 (1981).
[161]E. J. Kolmes, I. E. Ochs, and N. J. Fisch, Phys. Plasmas **25**, 032508 (2018).
[162]S. J. Zweben, N. J. Fisch, R. Gueroult, I. Ochs, C. A. Gentile, A. Khodak, and F. M. Levinton, "Overview of plasma mass filters for nuclear waste remediation, Princeton," Plasma Physics Lab Report No. PPPL-5444 (2018); available at https://bp.pppl.gov/pub_report/2018/reports-2018.html.